DELINEATING THE ROLE OF PROLACTIN-INDUCIBLE PROTEIN (PIP) IN BREAST CANCER LUNG METASTASIS

by

LUCAS EVANGELISTA DE LIMA TERCEIRO

A Thesis submitted to the Faculty of Graduate Studies of

The University of Manitoba

in partial fulfilment of the requirements of the degree of

MASTER OF SCIENCE

Department of Pathology

University of Manitoba

Winnipeg, Manitoba, Canada

ABSTRACT

In Canada, approximately 28,600 women were diagnosed with breast cancer (BC) in 2022, and about 40% of women currently fail primary management strategies and ultimately succumb to this disease. Despite many advances in the treatment of BC, metastatic relapse remains a major challenge for patients. The prolactin-inducible protein (PIP) is a highly breast specific gene product of BC. Because of such relevant attributes, it is considered a valuable BC biomarker frequently used in the clinic to determine the origin of an unknown metastatic carcinoma. However, the role of PIP in BC progression is still poorly understood. To address this role, our laboratory developed a novel transplantable mouse model of BC utilizing the 4T1-mouse metastatic BC cell line and determined that while over-expression of mouse homologous (Pip) suppressed tumor development in the primary tumor in the breast, it enhanced metastasis in lungs. We hypothesized that in the lung, Pip promotes a more aggressive phenotype in the BC cells. To further address this hypothesis *Pip*-expressing (4T1/Pip) and control BC cells (4T1/EV) were isolated from primary tumors and metastatic lungs of these mouse models and grown as *ex vivo* cell cultures. Several indicators of cellular transformation and metastatic progression were evaluated. Gene expression analysis of 4T1/Pip cells isolated from the metastatic lungs identified an up-regulation of genes involved in extracellular matrix disassembly, angiogenesis, positive regulation of cell migration and cell proliferation. Functional analysis studies showed that in the lungs, 4T1/Pip cells displayed increased proliferation, enhanced migration and colony formation compared to control. As well, morphological analysis of *ex vivo* cell cultures revealed that the 4T1/Pip BC cells developed a mesenchymal-like morphology compared to controls. Key EMT genes were also found up-regulated, whereas some epithelial markers were down-regulated in the 4T1/Pip cells from lungs. Furthermore, 4T1/Pip cells showed higher ERK1/2 phosphorylation

ratio and cell proliferation when cultured on a fibronectin-coated surface, suggesting that Pip may activate tumor progression pathways through fibronectin fragments interacting with membrane proteins. Collectively, these studies show that in the lung, *Pip*-expressing breast cancer cells acquire more aggressive traits consistent with the metastatic phenotype, suggesting that Pip may function differently in different tumor microenvironments. This work reveals a novel function of Pip in regulating breast cancer progression and metastasis.

ACKNOWLEDGEMENTS

I first need to express my greatest appreciation to my supervisors Dr. Yvonne Myal and Dr. Sabine Hombach-Klonisch. Thank you for seeing and believing in my potential, for having confidence in me and teaching me to have confidence in myself. I am also proud and extremely happy with all the valuable lessons, accomplishments, and personal growth I have experienced under your supervision. This work would not have been possible without your mentorship, support and guidance in training me.

I would also like to extend my gratitude to my committee members, Dr. Sam Kung and Dr. Kirk McManus for their excellent suggestions and contributions throughout this project. You have always been approachable and willing to help in all the times that I needed.

This project would not have been possible without the generous funding from many organizations: Natural Sciences and Engineering Research Council, The University of Manitoba Graduate Fellowship, The Research Manitoba & Cancer Care Master Studentship, and the MITACs Globalink Graduate Fellowship. Thank you for your financial support.

Thank you to Chidalu Edechi for your care and patience while training me when I first arrived in the lab and providing me with the necessary skills needed to thrive during my Master's program. To Matheus Fabiao, thank you for your friendship and for always being available to help me. Lastly, Barb Nickel, I can not express how appreciative I am of your help, patience, and friendship in the final steps of my master program. Thank you for always being excited about my project and new discoveries and for the huge efforts and commitment you made in trying to understand my project.

DEDICATION

This work is dedicated to Breast cancer survivors,

and to all cancer patients out there.

This is for you who are still fighting,

for you who won the battle, and for you who lost it.

ABBREVIATIONS

4T1	Transplantable mouse TNBC cell line
°C	Degrees Celcius
α5β1 integrin	"Fibronectin receptor"
4T1/EV	Control 4T1 cells containing empty vector
4T1/EV (1ºT)	4T1 control cells derived from primary tumor
4T1/EV (L)	4T1 control cells derived from metastatic lung
4T1/Pip	PIP expressing 4T1 cells
4T1/Pip (1ºT)	4T1 PIP expressing cells derived from primary tumor
4T1/Pip (L)	4T1 PIP expressing cells derived from metastatic lung
6-TG	6-thioguanine
A475nm	Absorbance at wavelength of 475 nM
AKT	Ak strain transforming
AKT2	AKT Serine/Threonine kinase 2
ALDH1	Aldehyde dehydrogenase 1
AR	Androgen receptor
ASCO/CAP	American Society of Clinical Oncology/College of American Pathologists
Asp	Aspartate
ATN-161	a5b1 integrin inhibitor
BALB/C	Mouse strain
BC	Breast Cancer
BCA	Bicinchoninic acid
BFC3H	Mouse strain

BL1 and BL2	Basal-like subtypes of TNBC
C3H	Mouse strain
CAF	Cancer associated fibroblast
CD24	Cluster of differentiation 24
CD4	Cluster of differentiation 4
CD44	Cluster of differentiation 44
CD45	Cluster of differentiation 45
cDNA	Complementary DNA
CK8	Cytokeratin 8
CMV	Cytomegalovirus
cMYC	Cellular-MYC a proto-oncogene
CO_2	Carbon dioxide
CRUMBS3	Crumbs protein homolog 3
CT	Cycle threshold
CTCs	Circulating tumor cells
CXCL12	C-X-C motif chemokine ligand 12
CXCL5	C-X-C chemokine ligand 5
CXCR2	C-X-C chemokine receptor 2
DAPI	4',6-diamidino-2-phenylindole
DC	Dendritic cell
DCIS	Ductal carcinoma *in situ*
DDR	Discoidin domain receptors
DMEM	Dulbecco's modified eagle's medium

DMSO	Dimethyl sulfoxide
DNA	Deoxyribonucleic acid
ECL	Enhanced chemiluminescence
ECM	Extra cellular matrix
EDTA	Ethylenediamine tetraacetic acid
EF1α	Elongation factor 1 alpha
EGF-1	Epidermal growth factor 1
eGFP	Enhanced green fluorescent protein
EGFR	Epidermal growth factor receptor
EMT	Epithelial-to-mesenchymal transition
EPCAM	Epithelial cell adhesion molecule
ER	Estrogen receptor
ERK1/2	Extracellular signal-related kinase 1 and 2
EV	Empty vector
FACS	Flow activated cell sorter
FAK	Focal adhesion kinase
FBS	Fetal bovine serum
FGF	Fibroblast growth factor
FN	Fibronectin
g	gravity
GAPDH	Glyceraldehyde-3-phosphate dehydrogenase
GCDFP-15	Gross cystic disease fluid protein
gp-120	Envelope glycoprotein 120

HDI	Human development index
HER2	Human epidermal growth factor receptor 2
HIV	Human immunodeficiency virus
HRP	Horseradish peroxidase
IL-10	Interleukin-10
IL-13	Interleukin-13
IL-1b	Interleukin-1 beta
IL-4	Interleukin-4
IL-6	Interleukin-6
ILK1	Integrin linked kinase 1
IP	Immunoprecipitation
JNK1	c-Jun N-terminal kinase
kDa	Kilodalton
KO	Knockout
LCIS	Lobular carcinoma in situ
LTBP-1	Latent TGF-b binding protein
M subtype	Mesenchymal subtype of TNBC
MAPK	Mitogen activated protein kinase
MCF-7	Human breast cancer cell line
MDA-MB-231	Human breast cancer cell line
MDA-MB-453	Human molecular apocrine breast tumor
MDSC	Myeloid derived supressor cell
MET	Mesenchymal to epithelial transition

mL	Millilitre
MLK3	Mixed lineage protein kinase 3
mM	Millimolar
MMP	Metalloproteinase
MMP-2	Metalloproteinase-2
MMP-9	Metalloproteinase-9
MMTV	Mouse mammary tumor virus
MOI	Multiplicity of infection
mRNA	Messenger ribonuceic acid
mSMGP	Mouse submaxillary gland protein
mTOR	Mammalian target of rapamycin
N	Number
N-cad	N-cadherin
NaCl	Sodium chloride
NOTCH	Neurogenic Locus Notch Homolog Protein
ns	Not significant
OD	Optical density
P	Probability
PAGE	Polyacrylamide gel electrophoresis
PARP	Poly-ADP ribose polymerase
PBS	Phosphate buffered saline
PCR	Polymerase chain reaction
PD-L1	Programmed cell death ligand-1

PDGF	Platelet derived growth factor
PI3Kα	Phosphoinositide 3-kinase alpha
PIP	Prolactin Inducible Protein (human)
PIP	Human gene of prolactin inducible protein
Pip	Mouse prolactin inducible protein
Pip	Mouse gene of prolactin inducible protein
PR	Progesterone receptor
RGD	Arg-Gly-Asp motif in FN-III
RIPA	Radioimmunoprecipitation assay
RNA	Ribonuceic acid
rpm	Revolutions per minute
RT	Room temperature
RT-qPCR	Real-time quantitative PCR
RTK	Receptor tyrosine kinase
s	Seconds
SD	Standard deviation
SDS	Sodium dodecyl sulfate
Src	Proto-oncogene tyrosine-protein kinase Src
STRING	Search Tool for the Retrieval of Interacting Genes/Proteins
T47D	Human breast cancer cell line
TAM	Tumor associated macrophage
TBS	Tris buffered saline
TBS-T	Tris buffered saline-Tween 20

TEC	Tumor endothelial cells
TGF-β	Transforming growth factor-beta
Th1	T helper, type 1
TME	Tumor microenvironment
TNBC	Triple negative breast cancer
TNF-α	Tumor necrosis factor-alpha
Treg	Reulatory T cells
TRIS-HCl	Tris-(hydroxymethyl)-aminomethane and hydrochloric acid buffer solution
v/v	Volume per Volume
V	Volts
VEGF	Vascular endothelial growth factor
VEGFR-1	Vascular endothelial growth factor receptor-1
VEGFR-2	Vascular endothelial growth factor receptor-2
w/v	Weight per Volume
XTT	2,3-Bis-(2-Methoxy-4-Nitro-5-Sulfophenyl)-2H-Tetrazolium-5-Carboxanilide
ZAG-2	Zinc alpha 2 glycoprotein
ZO-1	Zonula occludens protein 1
***μ*g**	Microgram
***μ*L**	Microlitre
***μ*M**	Micromolar

USED WITH PERMISSION AND CONTRIBUTION OF AUTHOR

PREFACE

This thesis contains material, images, and/or ideas from one article published in the peer-reviewed Cancers, of which Lucas E.L. Terceiro was co-first author. This journal applies the Creative Commons Attributions (CC BY) license to articles and other works, such that articles can be reused in whole or in part for any purpose.

CONTRIBUTION OF AUTHOR

INTRODUCTION: Figure 3

Terceiro, L. E., Edechi, C. A., Ikeogu, N. M., Nickel, B. E., Hombach-Klonisch, S., Sharif, T., ... & Myal, Y. (2021). The breast tumor microenvironment: A key player in metastatic spread. Cancers, **13**(19), 4798.

Contribution: Lucas E.L Terceiro contributed to original draft preparation (50%), editing (80%), and figure preparation (100%).

TABLE OF CONTENTS

LIST OF FIGURES

LIST OF TABLES

.

1. INTRODUCTION

1.1. BREAST CANCER

1.1.1. World and Canadian Statistics

BC is the second most frequently occurring cancer, and the most diagnosed cancer among women (World Cancer Research Fund, 2018; Sung et al., 2020). Worldwide, it affects more than 2.1 million women each year, accounting for more than 11.6% of all female cancers (Bray et al., 2021; Sung et al., 2020). The incidence of BC is significantly higher in developed countries, with an age-standardized incidence rate of 54.5 per 100,000 females while in nations with low to medium Human Development Index (HDI) the incidence is to 31.3 per 100,000 (Huang et al., 2021; Sharma et al., 2019; Fitzmaurice et al., 2018). Overall, BC mortality rate remains the highest in the female population, accounting for approximately 15% of all cancer-related deaths (Sung et al., 2020).

Similar to world statistics, in Canada, BC is the third most commonly diagnosed type of cancer, and the most frequent among the female population (Canadian Cancer Society, 2022). In 2022, an estimated 28,600 Canadians will be diagnosed with BC (Canadian Cancer Society, 2022), confirming this disease is the most common epithelial cancer and second only to lung cancer as the leading cause of cancer-related mortality among women in Canada (Brenner et al., 2020). Despite having a high incidence rate, the current overall five-year net survival rate for female BC is relatively high at 89% (Howlader et al., 2018). However, survival rates vary according to the stage and subtype, ranging from near 100% for stage I and 22% for stage IV (Azamjah et al., 2019; Waks et al., 2019).

1.1.2. Breast Cancer Progression and Subtypes

Clinical BC develops over a long period of time, requires several molecular alterations, and involves evolution of multiple cellular populations with increasingly aggressive phenotype characteristics. The current hypothesis for the natural development of BC is that it progresses from atypical ductal hyperplasia to ductal carcinoma *in situ* (DCIS), followed by evolution of this pre-invasive BC to invasive BC (Figure 1). DCIS is non-invasive, but it can vary from low-grade (non-life-threatening) to high-grade lesions that may contain invasive characteristics (Kurose et al., 2001).

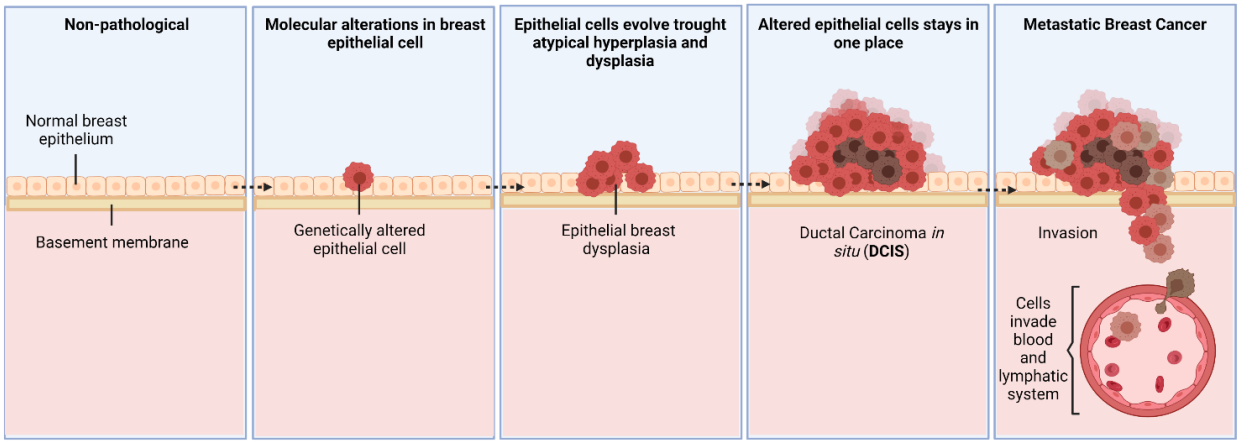

Figure 1 – Proposed stages of breast cancer progression. The classical multi-step model of human breast cancer progression is based on histomorphological and epidemiological data. Molecular alterations occurring in the epithelial cells of a normal terminal duct lobular unit result in atypical ductal hyperplasia/dysplasia. Subsequent molecular alterations can result in ductal carcinoma *in situ* (DCIS), another early neoplastic state, in which additional events can result in invasive ductal carcinoma.

BC is a very heterogeneous disease characterized by various pathological features with distinct therapeutic responses and patient long-term survival. As such, pathologists have defined many subtypes based on histological features. The majority of tumors belong to the invasive ductal carcinoma histological subtype (approximately 70 to 80% of newly detected tumors). The less

common subtypes include mucinous, cribriform, micropapillary, papillary, tubular, medullary, metaplastic, and inflammatory carcinomas (Weigelt et al., 2010); (Table 1).

Table 1 – Major histological subtypes of BC and their characteristics**.**

Histological Subtypes	Frequency (%)	5-year Survival (%)
Ductal Carcinoma *in situ* (DCIS)	3.6	>99
Lobular Carcinoma *in situ* (LCIS)	1.6	>99
Infiltrating (Invasive) Ductal Carcinoma	63.6	79
Infiltrating (Invasive) Lobular Carcinoma	5.9	84
Medullary Carcinoma	2.8	82
Inflammatory Breast Cancer	1.0	79
Mucinous Breast Cancer	2.1	95
Other	19.4	62

(Adapted from: http://p53.free.fr/our_work/breast.html)

Another classification used in the clinic is focussed on molecular subtypes. This is based on the presence or absence of expressed markers, namely: estrogen and progesterone receptor (ER, PR), as well as the human epidermal growth factor receptor 2 (HER2); (Tsang et al., 2020; Vuong et al., 2014). This classification is divided into 5 major subtypes: luminal A (ER^+, PR^+, $HER2^-$), luminal B (ER^+, PR^-, HER2 positive or negative), HER2-enriched (ER^-, PR^-, $HER2^+$) triple negative BC (TNBC) and the normal-like both which are ER^-, PR^-, $HER2^-$ tumors (Table 2) (Pusztai et al., 2006; Zepeda-Castilla et al., 2008). This categorization of BC is widely used to guide treatment choice and is also of prognostic value (Andre et al., 2006). For instance, ER^+/PR^+ tumors have a better prognosis than ER^-/PR^- tumors while $HER2^+$ tumors are more aggressive than $HER2^-$ tumors. In addition to the original classification, claudin status has been also used to subclassify BC, as a claudin low and high subtypes of BC have also been identified (Prat et al., 2010; Farmer et al., 2005; Blanchard et al., 2016).

Table 2 – Major molecular subtypes of BC

Molecular Subtype		Clinic-pathologic definition
Luminal A		ER^+, PR^+, HER2-, Ki-67 low (<14%)
Luminal B	HER2-	ER^+, PR^+, HER2-, Ki-67 high (>14%)
Luminal B	HER2+	ER^+, PR^+, $HER2^+$, any Ki-67
HER2+		HER2 over-expressed, ER^-, PR^-
Triple-Negative		ER^-, PR^-, $HER2^-$

1.2. TRIPLE NEGATIVE BREAST CANCER (TNBC)

1.2.1. Characteristics and Statistics

TNBCs are considered the most aggressive subtype of BC. TNBCs constitute 15–25% of all BCs and are naturally recurrent (Yam et al., 2017). The TNBC incidence in all age groups follows a trend, however younger and older women have increased rates of basal TNBC (Hudis and Gianni, 2011; Khan et al., 2017). TNBCs represent 24% of newly diagnosed BCs (Tsai et al., 2016), and there has been a steady increase in their incidence with 2,088,849 cases reported worldwide in 2018 (Singh et al., 2020). The clinical behavior of TNBC is relatively aggressive compared to the other subtypes of BC. TNBCs are considered a hard-to-treat BC, often displaying chemoresistance and increased distant recurrence with more frequent relapses and a higher incidence of metastasis (Dent et al., 2007). Because TNBC is highly metastatic, patients have a worse prognosis and higher recurrence rate when compared to other subtypes (Lehmann et al., 2011). The average survival rate in TNBC is ∼10.2 months with respect to currently available therapy, with a 65% 5-year survival rate in cases of regional tumors and 11% for those in which the tumor has already spread to distant organs (Kohler et al., 2015).

According to the American Society of Clinical Oncology/College of American Pathologists (ASCO/CAP) guidelines, TNBCs are classified by the cellular expression of ≤1% of

the progesterone and estrogen receptors and the expression of the human epidermal growth factor receptor 2 between 0 and 1+, as determined by immunohistochemistry (Bianchini et al., 2016; Wolff et al., 2014; Medina et al., 2020). There are four transcriptional subtypes of TNBCs: two basal subtypes (BL1 and BL2), a mesenchymal subtype (M), and a luminal androgen receptor subtype (Lehmann et al., 2016). TNBC can be further divided into six subgroups based on their molecular heterogeneity and deregulated pathway: immunomodulatory, luminal androgen receptor expression, mesenchymal stem-like, mesenchymal-like, basal-like 1, basal-like 2 (Table 3); (Yam et al., 2017). Populations of African American and Hispanic women are at high risk to develop TNBC, with African Americans as having a worse prognosis compared to other groups (Dietze et al., 2015; Sugita et al., 2016).

Table 3 – Molecular subtypes of TNBC

Molecular Subtype	Pathway
Immunomodulatory	Immune signaling
Luminal androgen receptor	AR
Mesenchymal stem-like	MET, TGF-beta, NOTCH
Mesenchymal	PI3K/AKT/mTOR
Basal-like 1	DNA damage repair
Basal-like 2	EGFR

1.2.2. Common metastatic sites for TNBC

Only 5% of patients with TNBC present with *de novo* metastatic disease (Yao et al., 2019). The majority of patients unfortunately relapse following treatment with curative intent. The biological features of TNBC result in a unique clinical phenotype. It is characterized by frequent metastasis to brain, bone, and visceral organs, primarily lung and liver (Table 4); (Lin et al., 2008; Edechi et al., 2020; Terceiro et al., 2021). Data from a Canadian BC cohort study of 180 TNBC

(total cohort = 1601) patients showed that TNBC patients were more likely to develop distant recurrence (HR = 2.6, P < 0.0001) or death (HR 3.2, P < 0.0001); (Dent et al., 2007). Although it is difficult to predict which secondary tissue will host the metastatic cells, recent studies found a correlation of specific gene patterns across several TNBCs and the most common distant metastatic sites (Anders et al., 2009; Yan et al., 2021).

Table 4 – Preferred metastatic sites for TNBC and non-TNBC. (Agarwal et al., 2016)

Site	TNBC	Non-TNBC	p-value
Bone	15.30%	16.20%	0.07
Lung	16.70%	8.80%	0.005
Liver	10.60%	9.30%	0.59
Brain	7.20%	3.00%	0.012
Chest Wall	5.90%	2.30%	0.016
Opposite Breast	2.50%	3.70%	0.41

1.2.3. Current management of TNBC

Common therapies for the management of patients with TNBC include surgery, radiotherapy, and systemic chemotherapy (Yin et al., 2020). From a therapeutic perspective, TNBC is very sensitive to chemotherapy, and for that reason, it is more commonly used. However, the treatments require extreme caution and daily care as it often becomes ineffective. Common treatments involve the use of alkylating agents (such as cyclophosphamide), anthracycline (doxorubicin, a topoisomerase blocker and DNA intercalating agent), anti-metabolite fluorouracil, and anti-microtubule agent (taxane) (Chang et al., 2019; Won et al., 2020). The choice of TNBC treatment, as for other BC subtypes, depends on the tumor stage.

1.2.4. Therapeutic options for early-stage TNBC

If TNBCs are diagnosed early, while the primary tumor is still small and has not yet metastasized, neoadjuvant therapy (most frequent taxanes and anthracyclines) with subsequent breast-conserving surgery or mastectomy is used (Almansour et al., 2022; Chalakur-Ramireddy et al., 2018). Neoadjuvant anthracycline and taxane-based chemotherapeutic regimens have remained the base of systemic therapy for early-stage TNBC and are mostly unchanged over the past years. The main paradox of early-stage TNBC neoadjuvant treatment is that although patients tend to achieve higher response to neoadjuvant therapy, they have a higher susceptibility for early disease recurrence with a tendency for visceral metastasis (Silva et al., 2022). Due to such observations, following neoadjuvant treatment and surgery intervention patients might also receive additional chemotherapy such as pembrolizumab, Olaparib or capecitabine to reduce the chances of cancer recurrence (Jhan and Andrecheck, 2017).

1.2.5. Therapeutic options for advanced TNBC

The treatment of advanced TNBC includes the following classes of drugs: anti-metabolites (gemcitabine and capecitabine), non-taxane microtubule inhibitor (eribulin), DNA cross-linkers (platinum, doxorubicin) and Poly-adenosine diphosphate Ribose Polymerase (PARP) inhibitor (Davison et al., 2021; Yoshida et al., 2014; Mckenna et al., 2017; Geenen et al., 2018). However, new therapies have been reported for advanced TNBC, particularly when surgery is not an option (Yin et al., 2020). Compared to other subtypes of BC, TNBCs show greater immunogenicity with tumor-infiltrating lymphocytes in the tumor microenvironment as well as expression of programmed cell death ligand 1 (PD-L1). Due to the therapeutic potential of the PD-L1 pathway, several immunotherapies have also been explored for TNBC as immune checkpoint inhibitors

(Nakhjanani et al., 2022; Lotfinejad et al., 2020). The goal of the use of immune checkpoint inhibitors is primarily to block regulatory immune checkpoints and consequently activate an anti-tumor response. This treatment strategy is considered a valuable option for TNBC and targets molecules that can negatively alter the immune response (Thomas et al., 2021). As such, the immune checkpoints can be quickly blocked by antibodies, such as atezolizumab combined with nanoparticle albumin-bound paclitaxel and pembrolizumab (Heimes et al., 2019; Schettini et al., 2016; Kwapisz et al., 2021). A recent phase 3 trial study, using atezolizumab in combination with nab-paclitaxel in patients with advanced TNBC, resulted in prolonged progression-free survival and overall patient survival (Gianni et al., 2022).

1.3. THE METASTATIC PROCESS

The metastatic development process is highly complex and poorly understood and includes multiple steps such as genetic and epigenetic alterations, angiogenesis, tumor–stroma interactions, intravasation through the basement membrane, survival in the circulation, and extravasation into distal tissues (Almansour et al., 2022; Anders et al., 2009).

It is a complex cascade of events facilitating the spread of cancer cells from the primary tumor site to distal organs. Proposed as the “seed and soil” hypothesis of cancer metastasis by Paget, cancer cells (seed) are thought to thrive at distant sites that provide favorable conditions (soil) where they prepare and alter the metastatic environment to ensure their survival (Paget, 1889).

1.3.1. Invasion and EMT

The metastatic process is believed to occur in 3 phases: invasion, intravasation and extravasation. During the invasion phase, the BC cells at the primary tumor site acquire aggressive features, which enable them to invade the basement membrane and escape the primary site (Lambert et al., 2017) (Figure 2). The process by which BC cells acquire aggressive features that facilitates tumor invasion is known as epithelial-to-mesenchymal transition (EMT) (Kotiyal et al., 2014; Bill and Christofori, 2015). The BC cells acquire mesenchymal characteristics which confer a migratory phenotype and stem cell-like properties (Derynck et al., 2019). Although previously thought to be a binary event by which cancer cells acquire either epithelial or mesenchymal phenotypes, recent studies demonstrate that EMT is much more complex (Zhang et al., 2018; Pearson et al., 2019). It has now been shown that some cancer cells possess a hybrid of both epithelial and mesenchymal phenotypes, that exhibit higher metastatic potential and chemoresistance compared to either "fully" epithelial or mesenchymal cancer cells (Sinha et al., 2020; Bornes et al., 2021; Liao et al., 2020). The transforming growth factor beta (TGF-β), released by tumor-associated macrophages (TAMs) and cancer-associated fibroblast (CAFs) in the primary tumor microenvironment (TME) play a key role in inducing EMT (Chen et al., 2018; Vakili-Ghartavol et al., 2018). Once released, the TGF-β upregulates expression of key transcription factors, Twist, Snail and Slug, which stimulate the EMT (Howley et al., 2019; Djediai et al., 2021). With the newly acquired mesenchymal phenotype, the cancer cells are now able to penetrate the blood vessel (intravasation) and enter the circulation.

1.3.2. Intravasation and CTC

Following intravasation, the BC cells are now referred to as circulating tumor cells (CTCs). CTCs are defined as a heterogenous group of tumor cells that were shed from the primary tumor and have entered the bloodstream (Cristofanilli et al., 2004). These cells are phenotypically and genetically distinct from the primary tumor cells, and generally express EMT and stem-like markers (EPCAM+, CK8+, TWIST1±, AKT2±, PI3Kα±, CD45-, ALDH1±, $CD44^{high}/CD24^{low}$) (Aktas et al., 2009; Al-Hajj et al., 2003). CTCs can be utilized as a diagnostic marker for metastatic BC. In fact, liquid biopsy with genomic and proteomic analysis has been considered a promising tool that will allow a clinical oncologist to determine the most suitable BC therapy (Mathai et al., 2019). BC cells have been shown to migrate into the circulation, either as single cells or as multicellular aggregates (referred to as collective migration) with the latter reported to possess a higher metastatic potential than the single cells (Cheung et al., 2016; Aceto et al., 2014). Factors expressed by BC cells such as plakoglobin and claudin 1 are reported to play key roles in facilitating their collective migration (Aceto et al., 2014; Zhou et al., 2015). The increased metastatic potential of multicellular aggregates is attributed to their ability to interact with stromal cells and survive the high-shear conditions in the circulation (Gkountela et al., 2019; Duda et al., 2010; Massague et al., 2016).

1.3.3. Extravasation and MET

Upon arrival at the secondary site, BC cells leave the vasculature (extravasation) and enter the distal site where they may remain as dormant cells to better adapt to the new microenvironment, or re-initiate secondary tumor growth when conditions become favorable (Lambert et al., 2017). Following extravasation, BC cells may revert from a mesenchymal to epithelial phenotype by

activating the mesenchymal-to-epithelial transition (MET), facilitating tumor establishment in secondary organs (Wells et al., 2008; Chao et al., 2012). Accumulating evidence suggests that MET may play a critical role in metastatic colonization by reactivating important cell signaling pathways and enabling attachment and interaction between cells and the extracellular matrix (ECM) within the host tissue (Wells et al., 2008; Chao et al., 2010; Stankic et al., 2013). When BC cells arrive in secondary organs, MET is activated, and BC cells then begin to re-express epithelial markers, such as E-cadherin, occludin and Crumbs3, and at the same time down-regulating mesenchymal transcription factors (Chao et al., 2010; Demirkan et al., 2013). This orchestrated intracellular process provides the necessary cellular machinery required for metastatic outgrowth (Demirkan, 2013).

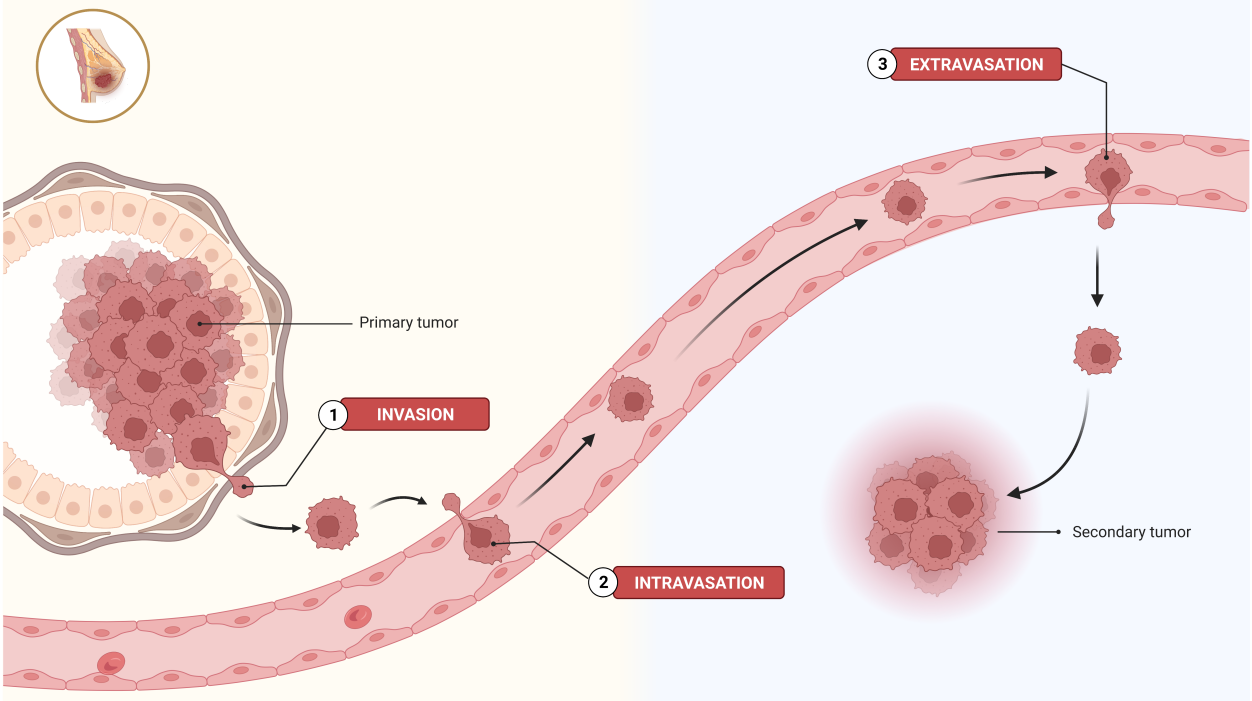

Figure 2 – The metastatic process. The initial step of metastasis requires the tumor to invade (**1**) through adjacent tissues and basement membranes. This process continues until individual tumor cells infiltrate (**2**) the blood vessels or lymphatic channels (intravasation) and are carried to a distant target tissue. The tumor cells then arrest in a small vessel within the distant organ, extravasate into the tissue and proliferate at the secondary site (**3**).

1.4. THE TUMOR MICROENVIRONMENT

1.4.1. Cellular components

In the primary tumor microenvironment, stromal cells are in constant contact with both BC cells and their secreted factors (Bussard et al., 2016). The effects of these interactions include changes in gene expression (such as metabolic reprogramming and EMT) not only in the TNBC cells, but also in neighboring stromal cells (Mbeunkui et al., 2009). The complex and multilayered crosstalk between BC cells and stromal cells within the microenvironment, such as tissue-resident and peripherally recruited immune cells, fibroblasts, endothelial cells, among others, greatly influences tumor progression. Changes occurring within the primary breast TME collectively favor

both TNBC cell survival and metastasis (Hill et al., 2020) (Figure 3). Below is a brief description of cellular components of the tumor microenvironment and their roles during tumor progression and metastasis.

1.4.1.1. Fibroblasts

In the stroma of the primary tumor, fibroblasts constitute one of the most abundant cell types. The exposure of mesenchymal stem cells to pro-inflammatory cytokines, tumor necrosis factor-alpha (TNF-α) and interleukin-1 beta (IL-1β) can lead to the development of the cancer-associated fibroblast (CAF) phenotype (Alkasalias et al., 2018). In general, CAFs secrete major cytokines including TGF-β1, C-X-C motif chemokine ligand 12 (CXCL12), platelet-derived growth factor (PDGF), interleukin-6 (IL-6) as well as extracellular matrix (fibronectin and collagen) which promotes tumor growth and metastasis (Jena et al., 2021; Luo et al., 2015; Yu et al., 2014).

1.4.1.2. Endothelial Cells

Within the primary tumor, a subset of endothelial cells, tumor endothelial cells (TEC), play a central role in BC development and progression. The interaction between BC cells and TECs have been shown to trigger angiogenesis, which increases nutrients and oxygen allowing the TNBC cells to survive the harsh tumor environment and increase their chances of spreading to distant sites (Madu and Johann, 2009; Nagl et al., 2020). In fact, studies showed that TECs isolated from primary and metastatic tumors show up-regulation of several angiogenesis-related proteins (VEGFR-1, VEGFR-2, and VEGF), as well as gelatinases/collagenases IV and MMPs (MMP-2 and MMP-9) (Ohga et al., 2012; Bussolati et al., 2006).

1.4.1.3. Immune Cells

Another component of the primary breast TME are the immune cells which can elicit both pro- and anti-tumor activity (Graney et al., 2021). The immune cells present in the breast TME are diverse with the most common being macrophages, which are an innate immune cell type (Hill et al., 2020). Macrophages play dual roles in the breast tumor environment depending on whether the macrophage is classically (M1) or alternatively (M2) activated (Muller et al., 2020). M1 macrophages produce proinflammatory cytokines with antitumor activity which contribute to BC clearance, whereas M2 macrophages produce anti-inflammatory cytokines supporting BC progression (Muller et al., 2020; Qiu et al., 2018; Aras et al., 2017). Tumor-associated macrophages, often M2 macrophages, promote the escape of primary tumor cells into the circulation by secreting epidermal growth factor-1 (EGF-1), TGF-β, IL-6, IL-10, and TNF-α, all of which promote EMT, and enhance the stemness of cancer cells, ultimately increasing invasiveness and migration into surrounding vasculature (Chen et al., 2018; Kitamura et al., 2015). Breast tumors can also avoid immune-mediated elimination, by stimulating M2 macrophage formation or upregulating PD-L1 expression (Fang et al., 2021). In the latter scenario, the binding of PD-L1 secreted by tumor cells to the PD-1 receptors of activated T lymphocytes leads to inactivation of cytotoxic T cells. Furthermore, a subset of innate immune cells, referred to as myeloid-derived suppressor cells (MDSCs) also contribute to metastasis in BC by secreting factors such as interleukin-10 (IL-10), TGF-β and VEGF which suppress the immune response, increase EMT and stimulate angiogenesis respectively (Ma et al., 2019).

The major adaptative immune cell subset is the regulatory B and T cells, which reduce the anti-tumor immune response in the TME, thereby promoting tumor progression (Weber et al., 2015). In the TME, regulatory T cells stimulate M2 macrophage survival and increase apoptosis

of anti-tumor cytotoxic T lymphocytes. Similar to their T cell counterparts, regulatory B cells have been shown to also promote tumor progression and metastasis (Olkhanud et al., 2011).

1.4.2. Non-cellular components

The non-cellular components, extracellular matrix proteins, of the tumor microenvironment, remain poorly understood and undervalued players in BC despite increasing evidence of their contribution to cancer progression (Kuroda et al., 2021). Composed of several extracellular proteins (fibronectin – FN, collagen, elastin, and laminin), the ECM is an important physical component of the tumor microenvironment (Kim et al., 2020). The ECM provides not only a physical scaffold for cells, but also serves as a depot for cytokines and growth factors such as VEGF, FGF, PDGF and TGF-β, which regulate tumor cell dissemination (Brassart-Pasco et al., 2020; Anderson et al., 2020).

1.4.2.1. Fibronectin

Fibronectin is a very important component of the ECM. Found as a dimer of 440 kDa, each subunit of fibronectin contains three types of repeating modules: FN-I, FN-II, and FN-III (Pankov et al., 2002). Fibronectin can bind to several cell surface receptors, stimulating cell proliferation, differentiation and supporting survival (Fernandez-Garcia et al., 2014). The fibronectin tripeptide Arg-Gly-Asp (RGD) motif located in FN-III interacts with the cell mainly through binding to the α5β1 integrin on the cell surface (Qiai et al., 2020; Akiyama et al., 1995). This interaction results in activation of several intracellular pathways, most commonly reported is the activation of ERK1/2, which translocates to the nucleus reducing sensitivity to apoptotic signals and promoting cell cycle progression (Lee et al., 2006; Hannigan et al., 2005). Additionally, the interaction of fibronectin and cancer cells can promote pro-oncogenic effects through the activation of

PI3K/AKT and focal adhesion kinase (FAK), which promotes proliferative signals, resistance to apoptosis and increased cell motility (Utispan et al., 2012; Lin et al., 2019). In fact, ATN-161, an α5β1 integrin inhibitor, is being evaluated in clinical trials as treatment for metastatic BC (Cianfrocca et al., 2006). It inhibits tumor growth and metastasis as well as extending survival in multiple animal tumor models, including BC, either when given as a single agent or when combined with chemotherapy or radiotherapy (Stoeltzing et al., 2003; Cianfrocca et al., 2006).

1.4.2.2. Collagens, Elastin and Laminin

Collagen, a component of the ECM, also influences BC cell behavior by inducing cancer cell invasion, proliferation, hypoxic regulation, intratumoral vessel regulation and metastasis. BC cells can re-shape the collagen network to form a reinforcing cell-collagen loop which progressively fosters cancer progression (Xu et al., 2019). Collagen filaments interacts with BC cells mainly by directly connecting to cell receptors. Discoidin domain receptors (DDRs) are a subfamily of tyrosine kinases that are divided in two homologous receptors (DDR1 and DDR2); (Favreau et al., 2014). Collagens can closely associate with DDRs and activate intracellular pathways that ultimately facilitate tumor progression and metastasis. The interaction of collagens with DDR2 have been reported to stimulate ERK2 in a Src-dependent manner; activated DDR2 then phosphorylates Snail1 resulting in glycogen synthase kinase 3 inhibition, ultimately contributing to sustained MMP-14 and collagen synthesis in BC (Zhang et al., 2013). The sustained activation of MMP-14 is one of the major factors that results in the ECM remodeling leading to tumor invasion.

Association of laminins and elastin with tumorigenesis in BC has also been established. Abnormal expression of laminins and elastin, which are frequently observed in the breast undergoing tumorigenesis, mainly results in disturbed cell behavior. Studies have provided

evidence that laminins can promote anchorage-independent cell growth, increase migration, and cell adhesion (Sevilla et al., 2010; Kusuma et al., 2012). Much as laminins, elastin also plays an important role during tumor progression. During BC tumor progression elastin can be degraded and elastin-derived peptides can affect tumor cells and their surroundings by promoting cell migration, up-regulation of MMPs, facilitating chemotaxis, angiogenesis, and modulating antiapoptotic pathways (Zakout et al., 2012; Wang et al., 2020).

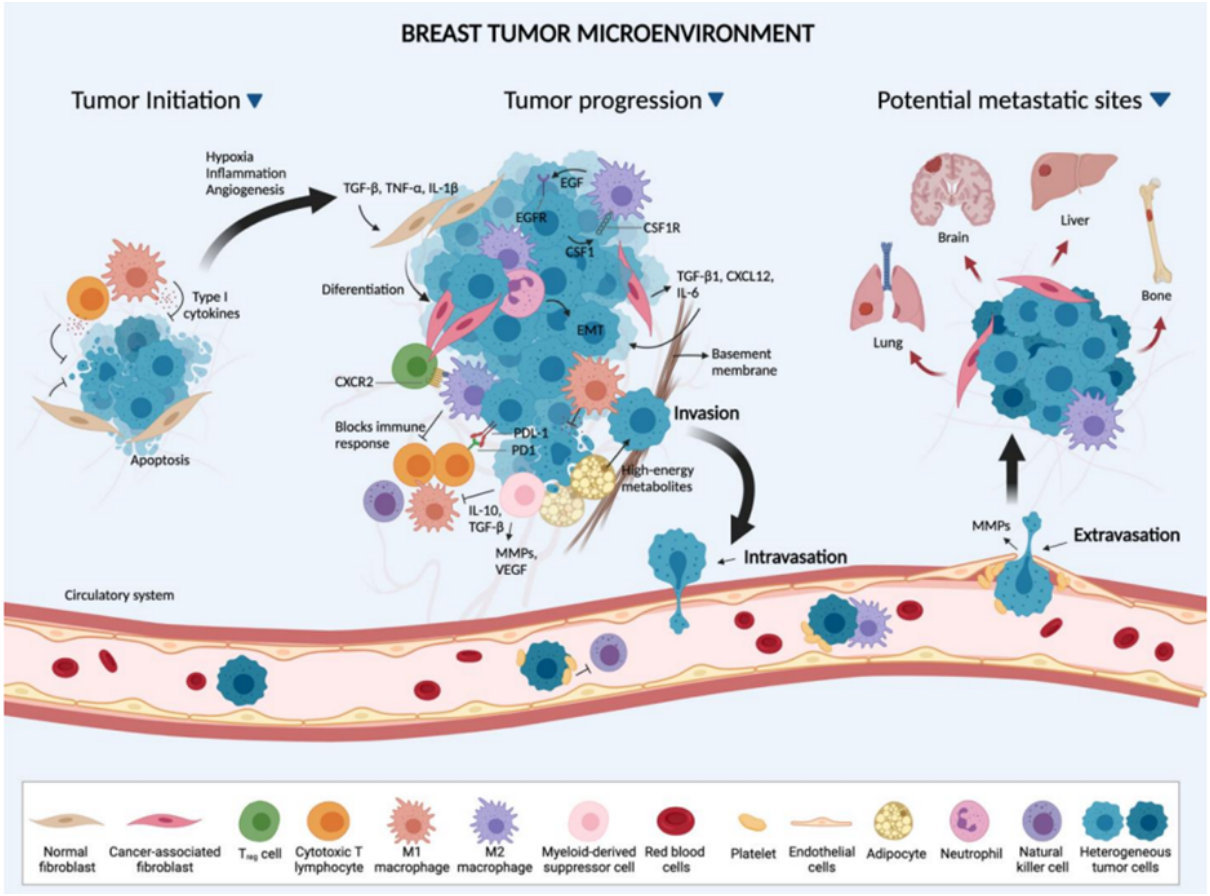

Figure 3 – The tumor microenvironment (TME) and breast cancer progression. At tumor **initiation**, growth-suppressive signals from the inflammatory process, primarily modulated by cytotoxic T-lymphocytes, M1 macrophages and fibroblasts are overcome by educating host stroma cells to acquire pro-tumorigenic features. Cytokines (TGF-β, IL-1β and TNF-α) released by the inflammatory process modulate differentiation of normal fibroblasts to cancer-associated fibroblasts (CAFs) which in turn, secrete extracellular matrix proteins and soluble factors (TGF-β, CXCL12, IL-6) that stimulate epithelial to mesenchymal transition (EMT), tumor growth and **progression**. Neutrophils induce EMT and promote tumor progression through cytokine release while adipocytes provide fuel for tumor growth. Tumor-associated macrophages (primarily M2 macrophages) support BC growth and ***invasion*** by secreting pro-tumorigenic cytokines and growth factors. During tumor expansion, activated cytokines in the environment (CXCL5-CXCR2, TGF-b) stimulate recruitment of regulatory T cells (Treg) and myeloid-derived suppressor cells (MDSCs) which disrupt immune surveillance by inhibiting cytotoxic T lymphocytes, M1 macrophages and natural killer cells. Also, BC cells escape immune surveillance by overexpressing the PD-L1 ligand. Such orchestrated events in the primary tumor allow tumor cells to acquire a mobile and invasive phenotype. Secreted factors (MMPs, VEGF) further facilitate tumor cells ***intravasation*** into the circulation. Once there, BC cells interact with platelets and M2 macrophages inhibiting immune recognition. Platelets escort tumor cells to secondary sites, where interaction with endothelial cells promotes **extravasation**. The preferred site of metastasis is influenced by the BC subtype. (Terceiro et al., Cancers 2021, 13, 4798)

1.5. THE PROLACTIN-INDUCIBLE PROTEIN (PIP)

The prolactin-inducible protein is a biomarker that has been associated with pathological conditions of the mammary gland. Pioneering studies by Shiu and Iwasiow (1985) initially identified PIP as a 15-17 kDa glycoprotein produced by the human BC cell line T47D, in response to prolactin stimulation. Independently, PIP was earlier identified as gross cystic disease fluid protein 15 (GCDFP-15), an abundant acidic protein mainly found in the fluid of gross cystic disease of the human breast (Haagensen et al., 1979). Currently, PIP/GCDFP-15 is routinely used in the clinic as a BC biomarker to confirm whether an unknown metastatic carcinoma originated from the breast (Calza et al., 2006; Dawood et al., 2011; Lund et al., 2010).

1.5.1. *PIP* Gene: Expression and Regulation

The human PIP protein is encoded by the *PIP* gene located on the long arm of human chromosome 7q34. The *PIP* gene is 7 kb long and contain 4 exons (Myal et al., 1991). The protein is comprised of 146 amino acids and contains a signal peptide of 28 residues. PIP is initially synthetized as a precursor polypeptide of 12.5 kDa and after maturation its size is reduced to 11 kDa. PIP can be found in three different protein size, 11 kDa, 14 kDa and 16 kDa in size, with the 14 kDa being the predominant isoform. Both the 14 kDa and 16 kDa are glycosylated versions of the 11 kDa protein (Figure 4); (Myal and Shiu et al., 2000).

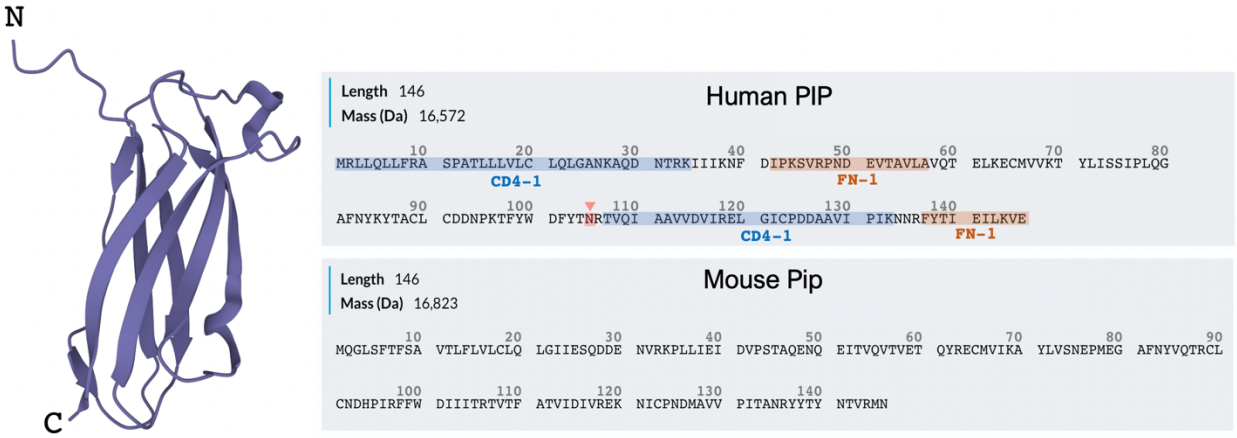

Figure 4 – The three-dimensional structure and amino acid sequence of prolactin inducible protein. The human PIP protein is composed of seven β-sheets with the site for the N-glycosylation at Asn105 (red arrow). The location of Fibronectin (FN) and CD4-binding domains are highlighted in orange and purple, respectively.

PIP is highly expressed in the cells of lacrimal, salivary and sweat glands (Hassan et al., 2009; Mazoujian et al., 1983). PIP is a secreted protein, found in specific bodily fluids such as tears, saliva and sweat, amniotic fluid, seminal plasm, and ear wax (Haagensen et al., 1979; Murphy et al., 1987; Autiero et al., 1991; Myal and Shiu, 2000). *PIP* expression is regulated by a number of hormones, with the highest levels induced by androgens, prolactin and glucocorticoids. As well, *PIP* is also regulated by cytokines, interleukin 4 and 13 (IL-4, IL-13) under both normal and pathological conditions of the breast (Shiu and Iwasiow, 1985; Blais et al., 1996).

1.5.2. PIP in innate and adaptative immunity

The function of PIP is only beginning to be elucidated. Previous evidence has pointed to a role in host defense and immune modulation. In healthy individuals, PIP is found strategically located at privileged immunological sites (ear canal, oral cavity, lacrimal gland and skin) predominantly in mucosal-type tissues that produce secretions responsible for the first line of defense from invading organisms, suggesting a role in innate immunity. Many studies support such a role, including one from the Myal research group which showed that oral-derived Pip in mouse saliva could bind and inhibit the growth of bacteria in the oral cavity (Lee et al., 2002).

PIP has also long been thought to play a role in adaptative immunity. It has been previously shown that PIP binds with high affinity to the CD4 molecule, a T-cell co-receptor molecule that plays a critical role in helping T-cell activation (Autiero et al., 1995, 1997; Zhou et al., 2003). Also, PIP interacts with envelope protein gp-120 of HIV-1, which is used by the virus to enter the $CD4^{+}$T immune cells (Autiero et al., 1997). Moreover, the crystalline structure of human PIP, also supports an immunomodulatory role for PIP, as numerous sites for the binding of immunoglobulins have been identified (Hassan et al., 2008). To establish a direct link between PIP and adaptative immunity, the Myal laboratory generated a *Pip* transgenic (Myal et al., 1998) and a *Pip* knockout (*Pip* KO) model (Blanchard et al., 2009) to conduct immunophenotypic analyses. It was observed that *Pip* KO mice had lower numbers of CD4+T cells, and defect in the activation of the T helper, type 1 (Th1) immune response (Li et al., 2015). Furthermore, Pip deficiency was also found to be associated with impaired intracellular signaling events in macrophages and dendritic cells (DCs), leading to the decrease in production of pro-inflammatory cytokines. Altogether, these studies revealed for the first time, that Pip is critical for optimal activation and function of cell-mediated immunity.

1.5.3. PIP in BC

In the normal breast tissue, the expression of *PIP* is low to undetectable. However, *PIP* expression is frequently increased in BC (Murphy et al., 1987; Fiel et al., 1996). Studies utilizing gene expression have detected *PIP* mRNA in 92% of the primary tumor tissues analyzed, which concurs with the level of PIP detected by immunohistochemistry (Clark et al, 1999). PIP levels were also found to be up-regulated in metastatic BC cells found in the axillary lymph node and in circulating tumor cells of BC patients (Clark et al., 1999). The highest levels of *PIP* mRNA were found in the luminal A molecular subtypes (ER+, PR+), whereas intermediate amounts were found in HER2-enriched and normal-like subtypes, with the lowest expression in basal-like subtypes (Baniwal et al., 2013; Naderi et al., 2014). As well, clinical evidence showed that BCs with high *PIP* expression displayed longer overall and disease-free survival (Hahnel et al., 1996; Pagani et al., 1994; Fritzsche et al., 2007). Furthermore, studies showed that high *PIP* expression correlated with a positive response to standard adjuvant chemotherapies (doxorubicin and cyclophosphamide) in a cohort of 120 invasive ductal carcinoma cases (Jablonska et al., 2016).

The crystalline structure of human PIP revealed a potentially multifaceted protein with a Zn^{2+} binding site, that has been demonstrated to tightly bind zinc alpha 2 glycoprotein (ZAG-2) a protein with strong antibacterial activity (Hassan et al., 2008). As well human PIP is an aspartyl protease (Caputo et al., 2000) with an aspartate residue at position 22 (Asp22), which shows homology to the aspartate residue 32 of other aspartyl proteases, such as cathepsin D, pepsin, and renin. In fact, PIP is be able to cleave fibronectin due to its aspartyl proteinase activity (Caputo et al., 2000; Hassan et al., 2008). This observation provided strong evidence that PIP can mediate ECM degradation, a key step in facilitating cellular transformation and metastasis during BC progression. PIP has also been shown to interact with several other proteins including actin,

fibrinogen, β-tubulin, serum albumin, and Fc fragment of immunoglobulin G (Naderi et al., 2014; Leon et al., 1994; Schenkels et al., 1991; Chiu and Chamley, 2003; Kumar et al., 2012). However, the biological role of such interactions remains unknown or poorly understood.

1.6. USE OF THE ORTHOTOPIC TNBC MOUSE MODEL TO ADDRESS PIP FUNCTION IN BC METASTASIS

To adequately study BC development and progression, it is important that the initial TNBC tumor is implanted into the corresponding tissue in the animal model (Rashid et al., 2014). TNBC tumors of orthotopic models grow in the organ of origin in their natural tumor environment. The interaction of TNBC tumor cells with the tissue-specific stromal cells, such as macrophages, fibroblasts, adipocytes, affects tumor growth, differentiation, and invasive capability (Mendes et al., 2020). The interaction with stromal cells as well as tissue-specific immune cells (B and T lymphocytes and Natural Killer cells) result in primary tumors similar to those of the original tissue (Yamaguchi et al., 2018). This makes orthotopic tumor models extremely relevant for the study of tumor development and progression. Moreover, orthotopic tumors can metastasize with specificities comparable to human TNBC tumors. Thus, orthotopic models are highly relevant preclinical models to study BC development, progression, and metastasis. The features of the 4T1 TNBC mouse model make it an excellent choice to study BC biology.

1.6.1. The 4T1 mouse cell line

The 4T1 cell line was originally derived from a subpopulation of a spontaneous mammary tumor of a mouse mammary tumor virus (MMTV) positive BALB/C mouse foster nursed on a C3H mother (BALB/BfC3H). The 4T1 murine BC animal model was originally developed by

Miller et al. (1983) to study metastatic tumor heterogeneity. 4T1 is a transplantable TNBC mouse cell line that can be grown *in vitro* as well as in BALB/C mice. When implanted orthotopically, 4T1 is highly aggressive TNBC cell line capable of spontaneous metastasis to several distant organs such as the lungs, blood, lymph nodes, liver, bone, and brain. Due to its resistance to 6-thioguanine (6-TG) treatment, metastatic 4T1 cells can be precisely quantified even in distant organs (Miller et al., 1983).

1.6.2. The 4T1 Pip-expressing TNBC mouse model

The Myal laboratory previously transduced mouse 4T1 cells to express the mouse Pip protein in order to address the role of PIP during tumor development and progression (Edechi et al., 2021). The *Pip* expressing 4T1 cells can be orthotopically injected into the mammary fat pad of BALB/C mice. These implanted cells are very tumorigenic and comparable to stage IV of human BC. Additionally, due to low immunogenicity of these cells the occurrence of inflammation and tumor rejection is minimal. The 4T1 cells grow into a primary tumor that becomes palpable a few days after implantation. After 2 to 3 weeks this primary tumor metastasizes similar to a human TNBC. After tumor metastasis, 4T1 cells are recoverable from both the primary tumor and metastatic sites, for further analysis.

2. STUDY RATIONALE

Preliminary data from our laboratory strongly suggested that in the primary tumor the immune system played a role in supressing tumor growth but that in the metastatic lung environment the expansion of *Pip*-expressing cells was independent of the immune system (Edechi et al., 2021). These observations suggest that the lung tumor environment may play a role in impacting the behaviour of *Pip*-expressing cells. Using a transplantable mouse model of TNBC, developed by our group, *Pip* expression in the primary tumor was found to delay tumor onset and reduce tumor growth due the activation of anti-tumor immunity (Edechi et al., 2021). Paradoxically, PIP expression was also associated with higher number of TNBC cells in the lungs independent of the immune system (Edechi et al., 2021).

3. HYPOTHESIS

Pip expression increases TNBC metastasis in the lungs by enhancing both the invasive properties and survivability of the TNBC cells while facilitating interaction with host stroma environment to promote cellular expansion.

4. STUDY OBJECTIVES

To investigate the effect of Pip on lung metastasis the following objectives were formulated:

1. Evaluate molecular and morphological changes in *ex vivo* cultures of *Pip*-expressing TNBC cells isolated from primary tumor and lung metastatic site.

2. Investigate intrinsic mechanisms by which *Pip* expression may promote TNBC cell metastatic behaviour.

5. MATERIALS AND METHODS

5.1. Generation of *Pip*-expressing lentivirus constructs

The lentivirus constructs for the *Pip* coding sequence and the empty vector (EV) controls were previously designed by Anne Blanchard from the Myal laboratory in collaboration with Dr. Sam Kung director of the Lentiviral Core Facility at the University of Manitoba. In the Pip vector design, the *Pip* coding region (ORF033474) was inserted under control of the elongation factor 1 alpha (EF1a) promoter. Enhanced Green Fluorescent Protein (eGFP) was used as a reporter gene under control of the cytomegalovirus (CMV) promoter. A similar vector was constructed but without the *Pip* coding sequence and used as an empty vector control (Figure 5). Both the Pip and Empty Vector constructs were packaged into lentiviral particles prepared for transduction by Vector Builder (Chicago, IL, USA).

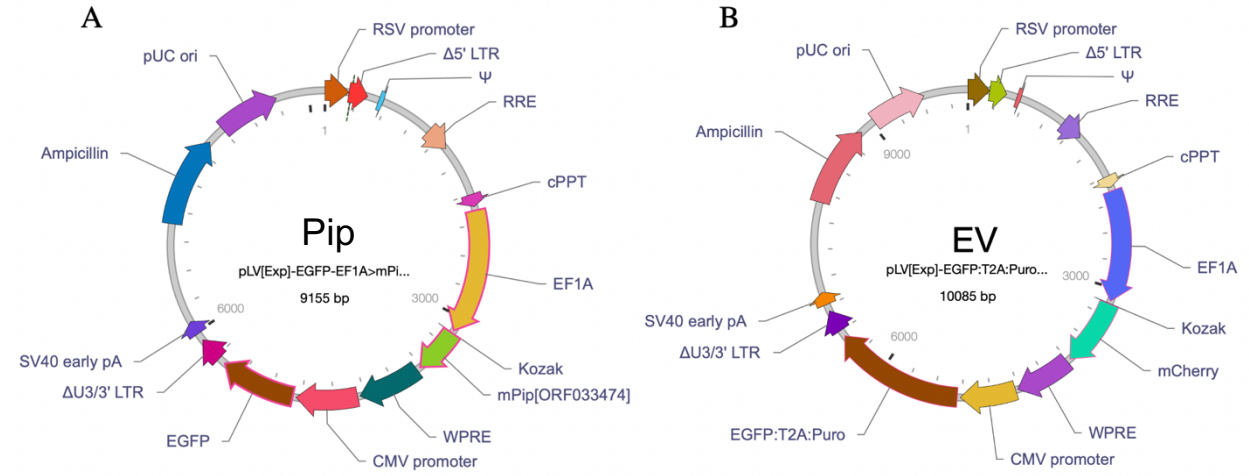

Figure 5 – Lentiviral vector constructs. (A) Shows the Pip lentiviral vector with mouse *Pip* coding region (ORF033474), represented as a green arrow, under EF1A promoter. (B) Shows the empty vector lentiviral control (EV) construct. The eGFP coding sequence is represented as a brown arrow in both constructs.

5.2. Lentiviral Transduction of 4T1 cells

Wild type 4T1 cell line was acquired from the American Type Culture Collection (ATCC, VA, USA). 4T1 cells were seeded in a 24-well plate at a concentration of $5x10^4$ cells/well and incubated overnight at 37 ^{0}C in a 5% CO_2 humidified incubator. The cell culture media (DMEM high glucose, 2 mM glutamine, 10% fetal bovine serum, 50 μg/ml streptomycin, 50 U/ml penicillin) was then completely removed and 250μL of media containing 20 MOI (multiplicity of infection) of virus and polybrene (5 μg/mL) was added to the plate and incubated at 37 ^{0}C for 12 h. Following incubation, the media-containing virus was safely discarded and replaced with 500 μL of fresh complete cell media. At 48-72 h after cell transduction, an inverted fluorescent microscope was used (Thermofisher Evos, Thermofisher, NY, USA) to visualize successfully transduced cells (eGFP+).

5.3. Cell Sorting

Since eGFP was used as protein reporter for successfully transduced cells, fluorescence-activated cell sorting (FACS) was used to separate the eGFP-positive cells from the eGFP-negative cells. Both 4T1/Pip and 4T1/EV cells were harvested using 0.05% Trypsin-EDTA and resuspended in flow cytometry buffer (1X PBS, 1% FBS and 2mM EDTA). Cell suspensions were passed through a 70 μm cell strainer to break up cell clumps. Cells were then collected, filtered and sorted based on eGFP expression using Flow Activated Cell Sorter (FACS) Aria II (BD Bioscience, CA, USA). Sorted cells were maintained in complete DMEM at 37 ^{0}C in a 5% CO_2 humidified incubator.

5.4. Mice

Six to eight weeks old BALB/C mice obtained from the in-house colony at the University of Manitoba, were used in this study. The mice were housed in the Central Animal Care Facility at the University of Manitoba, Canada, where they were maintained in a temperature-controlled room (22 ± 1 °C) with normal 12-h light/12-h dark cycle and fed *ad libitum*. All animal protocols were approved by the University of Manitoba Animal Care Committee and experiments were conducted according to the Canadian Council on Animal Care guidelines.

5.5. Implantation of transduced 4T1 mouse breast cancer cells

The 4T1/Pip and 4T1/EV cells were harvested from the culture flask using 0.05% Trypsin-EDTA for 5 min (Gibco, Grand Island, NY, USA) at 37 ^{0}C and 5% CO_2 (humidified incubator) and resuspended in a concentration of $1x10^4$ cells/100μL in cold 1X Phosphate Buffer Saline (PBS). Female BALB/C mice were placed inside a chamber and anesthetized with isoflurane 5%/oxygen until complete induction was achieved; anesthesia was maintained during procedure with 2.5%/oxygen isoflurane. After checking the animals for the absence of pedal and tail reflex, cells were orthotopically injected into the inguinal mammary gland using a 27G hypodermic needle following the established protocols of Pulaski and Ostrand-Rosenberg (2001); (Figure 6).

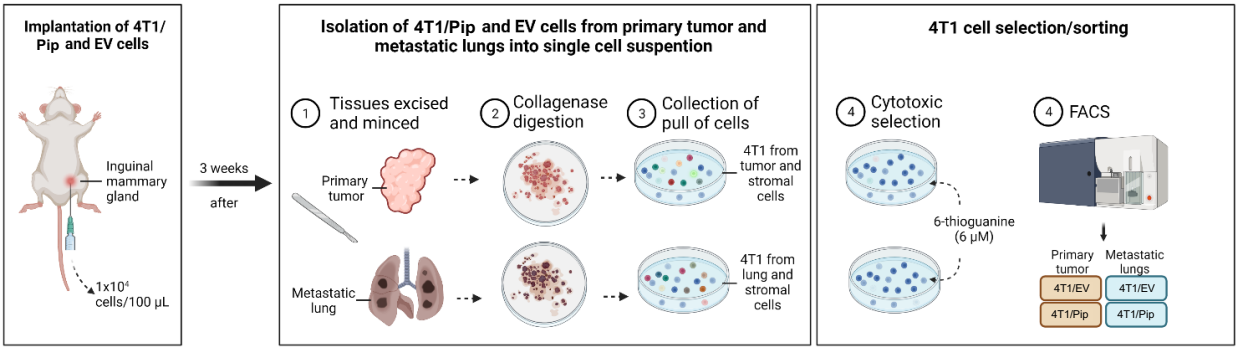

Figure 6 – Schematic representation of the isolation of 4T1/EV and 4T1/Pip *ex vivo* cultures. 4T1/Pip and EV cells were inoculated into the inguinal mammary gland of a BALB/C mouse. After 3 weeks of injection primary tumor (mammary gland) and lungs were excised. Tissues were digested using mechanical and enzymatic processes. After digestion 4T1 cells were sorted based on 6-thioguanine resistance as well as eGFP+ expression using FACS.

5.6. Generation of *ex vivo* cell culture of 4T1 cells

At 3 weeks post-inoculation of 4T1/Pip and 4T1/EV cells, tumor bearing mice were euthanized by cervical dislocation and the primary mammary tumor and lungs were excised. The tissues were minced with scissors and digested with 2 mL of collagenase IV solution (1.5 mg/mL, Millipore Sigma, Merck, MA, USA) for 1-2 hours. Digested tissues were passed through 40 µm Falcon cell strainer to obtain single cell suspensions. The cells were pelleted by centrifugation (500 x g for 10 min), resuspended in 10 mL of complete DMEM with 60 µM of 6-thioguanine and transferred to a 10 cm cell culture dish. Cell cultures were incubated for 10-14 days at 37 ^{0}C in a 5% CO_2 humidified incubator. It is expected that only 4T1 cells will grow under 6-thioguanine treatment; any other cells types would be eliminated while the 4T1 cells are able to survive. For further analysis the 4T1 cells derived from the primary tumor and metastatic lungs, both 4T1/Pip and 4T1/EV, were further enriched using FACS as they both express the reporter gene eGFP (Figure 6).

The *ex vivo* cultures of 4T1/Pip and 4T1/EV cells from primary tumor and lungs were maintained in high-glucose Dulbecco's Modified Eagle's Medium (DMEM; 4.5 g/l glucose, Hyclone Laboratories Inc., UT, USA) supplemented with 2 mM glutamine, 10% fetal bovine serum (FBS), 50 μg/ml streptomycin, 50 U/ml penicillin (all obtained from Hyclone Laboratories Inc., UT, USA) and 10 μg/ml bovine insulin (Sigma-Aldrich Canada, ON, Canada) and maintained at 37 ^{0}C and 5% CO_2 (humidified incubator). Cells were passaged every 2 days or at 85-100% confluency (as evaluated by brightfield microscopy). For passaging, cells were harvested as follows: T25 tissue culture flask (Thermofisher, NY, USA) was rinsed with 3ml of 1X phosphate buffered saline (PBS) and treated with 2ml 0.05% Trypsin-EDTA (Gibco, Grand Island, NY, USA) for 5 minutes or until cells were detached, 4 mL of complete DMEM was then added to inactivate the trypsin and the cells dispersed by pipetting 3-5 times before plating in a new T25 flask at a 1:6 subcultivation ratio.

To prepare cells for cryopreservation, cells were harvested as described above and centrifuged at 500 x g (IEC Centra-GP8R, International Equipment Company, MA, USA) for 10 minutes at room temperature. The cell pellets were resuspended in FBS containing 5% dimethyl sulfoxide (DMSO, freezing media) and aliquoted into cryopreservation vials (1ml/vial). Vials were transferred to a Styrofoam box which allows a more gradual decrease in temperature and then stored at -80 ^{0}C for at least 2 days before long term storage in liquid nitrogen tanks.

5.7. Western Blot analysis

***Sample preparation*:** Cells were grown to confluency in 6-well plates, then detached using a cell scraper in the presence of media, transferred to a 1.5 mL tube, pelleted by centrifugation, and washed one time with 1X PBS. Cells were lysed using 100 μL RIPA Lysis and Extraction Buffer (Thermofisher Scientific, NY, USA) containing protease inhibitor (Roche Diagnostics) and 1X Halt phosphatase inhibitor cocktail (Thermofisher Scientific, NY, USA), sonicated for 15 seconds, and centrifuged at 13000 rpm for 10 mins at 4 °C to remove insoluble material. The supernatants were transferred to a new tube and the protein concentration of the cell lysates determined using the Bicinchoninic acid (BCA) assay kit (Pierce Biotechnology) according to manufacturer's instructions. The cell lysates were stored at -20 °C to be used for sodium dodecyl sulfate-polyacrylamide gel electrophoresis (SDS-PAGE).

***SDS-PAGE*:** 20 μg of cell lysate was mixed with 2X Laemmli Sample Buffer (65.8 mM Tris-HCl, pH 6.8, 2.1% SDS, 26.3% (w/v) glycerol, 0.01% bromophenol blue and 0.05% (v/v) of β-mercaptoethanol) in a 1:1 ratio (v/v) and heated at 70°C for 10 minutes. Sample proteins as well as molecular weight markers (BioRad, ON, Canada) were separated by SDS polyacrylamide gel (5% acrylamide/bis-acrylamide for stacking gel and 10% acrylamide/bis-acrylamide for resolving gel) and run for 30 minutes at 90V followed by 60 minutes at 110V. Following electrophoresis, proteins were transferred to nitrocellulose membranes (0.45μm) (Bio-Rad Laboratories, Mississauga, ON, Canada) using Pierce™ 1-Step Transfer Buffer and the Pierce Power Blot Cassette (Thermo Scientific, NY, USA) for 7 minutes at 25V. Following transfer, the nitrocellulose membrane was blocked with 5% non-fat milk in Tris-buffered saline (20 mM TRIS, 0.15M NaCl) with 0.1% Tween-20 (v/v, TBS-T) for 1 hour. Primary antibodies were diluted in blocking solution according to Table 5, and incubated with shaking overnight at 4°C. The next day the membranes

were washed with TBS-T three times for 10 min each before adding the secondary antibody (Table 6) and incubating with a shaking for 1 hour at room temperature. Blots were washed with TBS-T three times for 10 mins and developed using enhanced chemiluminescence (ECL) kit (Immobilon, Millipore, MA, USA). Chemiluminescent signal was acquired using the C-digit blot scanner (Licor, NE, USA).

Table 5 – List of primary antibodies used for Western Blot analysis.

Antigen	Host	Dilution	Source	Cat. No.
ZO-1	Rabbit	1:2000	Thermofisher Scientific	61-7300
E-Cadherin	Mouse	1:1000	Thermofisher Scientific	MA5-12547
Vimentin	Mouse	1:500	Cell Signaling Technology	3390
ERK1/2	Rabbit	1:1000	Cell Signaling Technology	4695
p-ERK1/2	Rabbit	1:1000	Cell Signaling Technology	8544
Pip	Rabbit	1:2500	Alpha Diagnostics	n/a
α-tubulin	Mouse	1:5000	Abcam	ab7291

Table 6 – List of secondary antibodies used for Western Blot analysis.

Antibody	Host	Dilution	Source	Cat. No.
Anti-Rabbit (HRP)	Goat	1:1000	Thermofisher Scientific	A16116
Anti-Mouse (HRP)	Rabbit	1:1000	Cell Signaling Technology	D3V2A

5.8. Reverse Transcription quantitative real-time PCR (RT-qPCR) assay

RNA was extracted from cell samples (4T1/EV and 4T1/Pip from primary tumor and metastatic site) using Monarch Total RNA Miniprep Kit (New England BioLabs Ltd., ON, Canada) and quantified using a NanoDrop spectrophotometer (Nanodrop 2000, Thermofisher Scientific, NY, USA). LunaScript RT SuperMix (New England BioLabs Ltd., ON, Canada) was used to reverse transcribe equal amounts of RNA, according to manufacture's suggested protocol. The cDNA samples were applied to each real-time PCR reaction on the mouse tumor metastasis RT^2 Profiler PCR array (Qiagen Corporation, Mississauga, ON, Canada; cat# PAMM-028Z). Real time PCR was carried out using the CFX 96 RT-qPCR system (BioRad, ON, Canada). The cycle profile consisted of initial cDNA denaturation at 95°C for 10 min, followed by 40 cycles of 95°C for 15 seconds and 60°C for 1 min. The collected data were analyzed using the web-based PCR Array Data Analysis Software (Qiagen, ON, Canada). Up-regulated genes were input on the STRING database to find the related biological processes.

RT-qPCR analysis was also used to evaluate the expression of EMT markers. Following the manufacturer's instructions, the Luna Universal qPCR Master Mix (New England BioLabs Ltd., ON, Canada) was used with cDNA and gene specific primers. Thermal cycling profile consisted of polymerase activation and DNA denaturation at 95°C for 1min, followed by 40 cycles of 95°C for 15s and 60 °C for 60s (CFX 96 qPCR system, BioRad, ON, Canada). Cycle threshold and relative quantification values were calculated automatically by the CFX96 instrument software. Data were analyzed using the delta-delta CT method and presented as fold increase in gene expression levels relative to the house keeping gene, GAPDH. Primer sequences for genes analyzed are shown in Table 7.

Table 7 – Primer sequences used in qPCR assay.

Gene	Forward 5' – 3'	Reverse 5' – 3'
Vimentin	CGGAAAGTGGAATCCTTGCAGG	AGCAGTGAGGTCAGGCTTGGAA
Twist	AGCAGTGAGGTCAGGCTTGGAA	ACACGGAGAAGGCGTAGCTGAG
Snail	TGTCTGCACGACCTGTGGAAAG	CTTCACATCCGAGTGGGTTTGG
Slug	TCTGTGGCAAGGCTTTCTCCAG	TGCAGATGTGCCCTCAGGTTTG
N-Cadherin	CCTCCAGAGTTTACTGCCATGAC	CCACCACTGATTCTGTATGCCG
GAPDH	CATCACTGCCACCCAGAAGACTG	ATGCCAGTGAGCTTCCCGTTCAG

5.9. Fluorescence microscopy of 4T1 *ex vivo* cell cultures

The *Pip*-expressing 4T1 (4T1/Pip) and control cells (4T1/EV) retrieved from both primary tumor and metastatic sites were seeded and left for 12 hours on 8-well chamber glass slides (iBIDI) prior to fixing in 3.7% formaldehyde / 1x PBS for 10 minutes (RT). The slides were washed three times in 1X PBS (RT) for 5 minutes, with shaking, followed by incubation with 0.1% Triton X-100, for 12 minutes (Millipore Sigma, Merck, MA, USA). For F-actin staining, slides were incubated with 200 μL of Phalloidin-Alexa 488 (Thermofisher Scientific, NY, USA) working solution (5 unit/mL) in the dark for 30 min (RT) and washed with 1X PBS after incubation. The DNA was counterstained with DAPI (0.1μg/mL), for 5 minutes and the slides mounted using Vectashield (Vector Laboratories Inc, Burlingame, CA, USA). The images were taken using Zeiss LSM 710 AxioObserver microscopy system equipped with 20x/0.8 N.A objective lens (Andor, Oxford, UK). Images were acquired using 2% laser power, DAPI was excited using a 405 nm laser and Phalloidin used a 488 nm laser.

5.10. Cell counting: Trypan Blue Exclusion

The *Pip*-expressing 4T1 and control cells, derived from both the primary tumor and the lung metastatic site were seeded into a 12-well plate at a density of $5x10^3$ cell per well and cultured under standard conditions. Every day over 4 days, cells from three wells were detached using 0.05% trypsin (Hyclone Laboratories Inc., UT, USA) mixed with trypan blue (1:1) and counted using a TC-10 automatic counter (BioRad, ON, Canada).

5.11. Cell proliferation assay: XTT (Tetrazolium salt dye)

The XTT cell proliferation assay kit (ATCC, VA, USA) is a metabolic assay that indirectly measures cell proliferation when used according to manufacturer's instruction. XTT is a bright orange solution that, when metabolized by live cells, turns dark blue. Briefly, 4T1 *Pip*-expressing and control cells were seeded into a 96-well plate at density of 500 cell per well and cultured under standard conditions. Each day, for a period of 4 days, XTT was added to the culture media of 3 wells and incubated for 4 hours. Following incubation, the media was transferred into a new plate and the optical density measured at wavelength of 475nm and 660nm using a SpectraMax 190 (Molecular Devices, CA, USA.). The specific absorbance of the sample was expressed mathematically as: $OD = A_{475nm(Test)} - A_{475nm(Blank)} - A_{660nm(Test)}$.

5.12. Cell migration assay

To evaluate cell migration rate, a 3D cell spheroid assay was utilized. This assay most accurately reflects some of the characteristics of the tumor microenvironment, including nutrient and oxygen gradients, cell-cell interactions, necrotic core, quiescent zone, and proliferating edges.

To assess the migration rate of cells isolated from primary tumor and metastatic lungs, cells were harvested and cultured in 20 μL drops of complete media (500 cells per drop) suspended from the lid of a culture dish and allowed to generate the cell spheroids. After 72 hrs, using a 1 mL pipettor with a wide bore tip, spheroids were transferred to a 24-well plate (1 spheroid per well) and cultured with DMEM containing 1% FBS under standard culture conditions. Images were captured at 0, 6 and 20 hours after incubation using a microscope with a 5x objective attached to a camera (ScopePhoto 3.0, ScopeTek DCM Microscope Camera). The migration area was analysed and quantified using the ImageJ software (NIH). The migration area was represented as the final migration area (total area) minus the initial spheroid area at time zero (0).

5.13. Colony formation assay

Cell spheroids generated from 4T1/Pip and control cells isolated from both primary tumor and metastatic lungs were transferred to 12-well plates containing 2 mL of media (DMEM with 1% FBS). Following 2 weeks of incubation, the cells were fixed with 3.7%formaldehyde / 1xPBS for 10 minutes (RT), washed once with 1X PBS, and stained with Acridine Orange Staining Solution (0.05% v/v) for 10 min. The cells were then rinsed with 1X PBS. Images of the cells were then taken using an EVOS FLoid Imaging System (Thermofisher Scientific, NY, USA) and colonies were manually quantified using ImageJ software (NIH).

5.14. Fibronectin assay

A stock solution of fibronectin native protein (1 mg/mL, Gibco, Grand Island, NY, USA, #PHE0023) was diluted in 1X PBS to a working solution with a final concentration of 2 μg/mL. This “fibronectin working solution” was added to 6-well plates (1mL/well) and 96-well plates (50

μL/well) and left for 2 hours at 2-4 °C. The remaining solution was removed, and the plates left to dry for 10 min at room temperature. The fibronectin coated plates were used to grow 4T1 cells that were used for both protein analysis (6 well plates) and proliferation assays (96 well plates).

5.15. Statistical analysis

Statistical analyses were performed using GraphPad Prism 8.0 (GraphPad Software, Inc., San Diego, CA). Results are shown as mean ± SD. Two-tailed Student's t-tests, ANOVA or Mann Whitney tests were utilized to compare the means from different groups of cells. Differences between groups were considered to be significant at P value of <0.05.

6. RESULTS

6.1. Detection of Pip in 4T1 cells isolated from primary breast tumor and metastatic lungs

Western blot analysis was used to evaluate whether the metastatic process had impacted *Pip* expression levels in the 4T1 cells isolated from both the primary tumor and lungs. Cell lysates were prepared for Western blot analysis as outlined in "Material and Methods".

Using a polyclonal antibody to Pip, a 17 kDa band was identified in cells from both the primary tumor and lungs, but not in the corresponding empty vector control cells from the primary tumor and lungs. There were no significant changes in protein levels between *Pip*-expressing cells from the primary tumor and lungs (Figure 7).

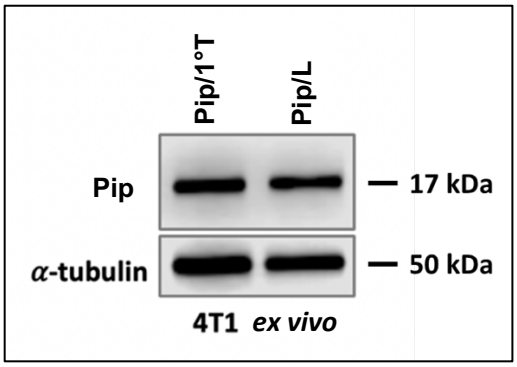

Figure 7 – Pip levels in *ex vivo* cells (4T1/Pip) derived from primary breast tumor and metastatic lungs are comparable. Cell lysates from 4T1/*Pip* expressing cells derived from primary tumor (Pip/1°T) and metastatic lungs (Pip/L) were analyzed by Western blotting using a rabbit anti-mouse PIP antibody. A 17 kDa band of similar intensity is observed in cells derived from both tissues. Loading control is α-tubulin (50 kDa).

6.2. Breast cancer metastatic gene expression analyses

To gain insight into how expression of *Pip* enhances metastasis to the lung, the expression of genes related to BC metastasis process were evaluated in both Pip-expressing (4T1/Pip) and non-expressing (4T1/EV) cells isolated from the primary tumor as well as the metastatic lung, using the RT² Profiler PCR array (Qiagen).

Table 8 – Gene Table: RT² Profiler PCR Array

Gene Symbol			
Ctnna1	***Mmp9***	*Hgf*	*Mta1*
Cdh1	*Timp2*	*Igf1*	*Smad4*
Cdh11	*Timp3*	*Ccl7*	*Tcf20*
Cdh6	*Timp4*	*Cxcl12*	*Chd4*
Cdh8	*Col4a2*	***Tnfsf10***	*Ewsr1*
Fat1	*Hras*	*Cxcr4*	*Smad2*
Nf2	*Il1b*	*Ephb2*	*Ctbp1*
Cd44	*Kras*	*Fgfr4*	*Ctsk*
Sgrey5	*Tgfb1*	*Flt4*	*Ctsl*
Itgb3	*Vegfa*	*Cxcr2*	*Elane*
Rpsa	*Brms1*	*Met*	*Fxyd5*
Apc	*Cdkn2a*	*Nr4a3*	***Hpse***
Fn1	*Pten*	*Lpar6*	*Htatip2*
Gpnmb	*Rb1*	*Plaur*	*Cd82*
Mtss1	*Trp53*	*Rorb*	*Mcam*
Mmp10	*Mdm2*	*Sstr2*	*Nme1*
Mmp11	*Kiss1r*	*Tshr*	*Nme2*
Mmp13	***Il18***	*Denr*	*Nme4*
Mmp2	*Kiss1*	*Mycl*	*Pnn*
Mmp3	*Myc*	*Src*	*Set*
Mmp7	*Csf1*	*Etv4*	*Syk*

It was observed that out of 84 metastasis-related genes (Table 8), 6 were upregulated in the 4T1/Pip cells from the primary tumor (bold) while 14 were upregulated in 4T1/Pip cells isolated

from metastatic site when compared to the respective 4T1/EV control cells (underlined). The up-regulated genes were narrowed down to their biological-related processes using the STRING database (https://string-db.org). The 4T1/Pip cells isolated from the metastatic lung showed an increase in cellular processes related to angiogenesis, extracellular matrix organization and disassembly, positive regulation of cell migration, extracellular matrix disassembly and regulation of cell population (proliferation), relative to control (Figure 8).

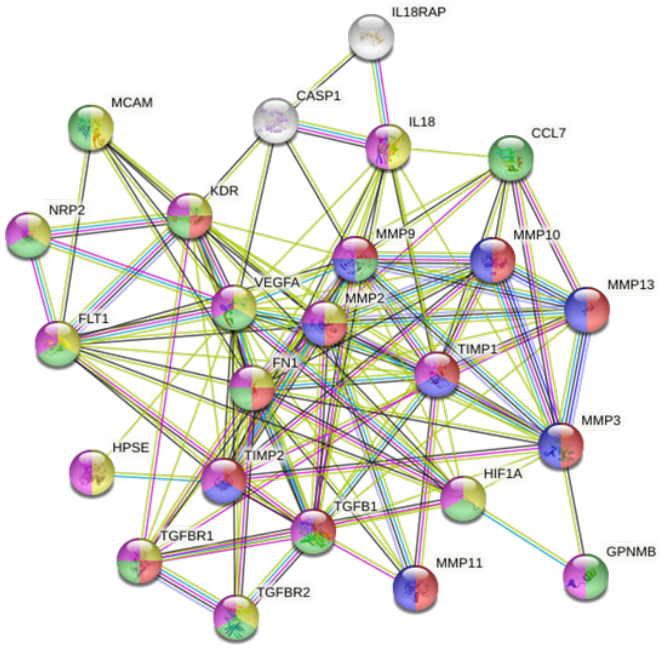

Pathway ID (GO)	Pathway description	False Discovery Rate
GO:0001525	Angiogenesis	4.31e-13
GO:0030198	Extracellular matrix organization	4.31e-13
GO:0030335	Positive regulation of cell migration	5.18e-13
GO:0042127	Extracellular matrix disassembly	9.64e-13
GO:0042127	Regulation of cell population proliferation	1.46e-10

Figure 8 – Biological-related processes of up-regulated genes in 4T1/Pip cells isolated from metastatic lungs. (A) STRING network analysis of up-regulated genes differentially expressed in 4T1/Pip cells isolated from metastatic lungs. The identified up-regulated genes were entered into the STRING database (https://string-db.org). Proteins are represented as nodes, with node colors representing different pathways in which proteins are involved (B). The STRING confidence level was set to 0.4 (medium).

6.3. *Pip*-expressing 4T1 cells undergo morphological changes during lung metastasis

Both 4T1 *Pip*-expressing and control cells isolated from both the primary breast tumor and the metastatic lungs were analyzed by confocal microscopy to investigate whether *Pip*-expression affects 4T1 cell morphology during metastatic dissemination.

No differences in cell shape between 4T1 *Pip*-expressing cells and 4T1/EV control cells isolated from primary tumor (Figure 9A and B) were observed. However, with the *Pip*-expressing cells a higher number of micro nuclei was noted. Distinct morphological differences were seen between control cells and those expressing Pip, isolated from the metastatic lungs. Figure 9C, shows that control cells from lungs maintained their original epithelial morphology with a polygonal shape, regular dimensions, cytoplasmic membrane spread across the surface, and attachment to neighboring cells. In contrast, Pip-expressing cells from lung displayed a mesenchymal morphology with spindle-shaped cells, a loss in physical cell-cell interaction, smaller nuclei, and less cytoplasm (Figure 9D).

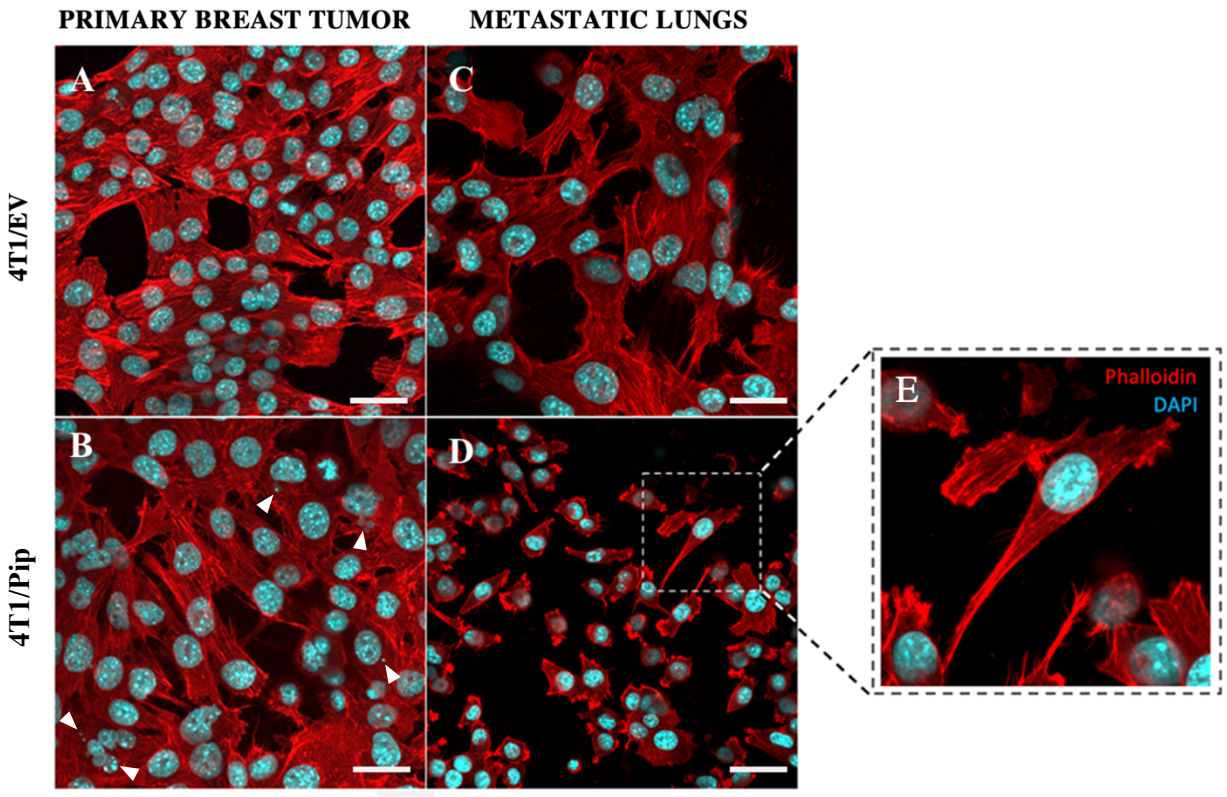

Figure 9 – Morphological changes in *ex vivo Pip* expressing cells isolated from metastatic lung. Both *ex vivo* control cells (4T1/EV) (A) and *Pip* expressing cells (4T1/Pip) (B) from the primary tumors, display epithelial morphology. However, *ex vivo* cells from metastatic lungs, control cells (C) display epithelial morphology whereas *Pip* expressing cells (D) show a mesenchymal morphology (E) Amplification of picture D. Scale bar, 50 μm. Red: Phalloidin-Alexa 488, Blue: DAPI. White arrow = micro nuclei.

6.4. *Pip*-expressing 4T1 cells isolated from metastatic site in the lungs exhibited enhanced proliferation

To evaluate whether Pip impacts cell proliferation in the primary tumor or at the metastatic site, two different approaches were used. The first approach was cell counting using the trypan blue exclusion assay. The second approach was to indirectly measure cell growth based on metabolic activity using the XTT assay (described in "Material and Methods"). From the results shown in Figure 10A, no significant difference was observed in growth rate between the *Pip*-expressing and control cells derived from the primary tumor with either assay (cell counting and XTT assay). However, in the cells isolated from the metastatic site (Figure 10B), a higher proliferation rate was observed in the 4T1 *Pip*-expressing cells compared to the control cells using both trypan blue exclusion and XTT assay. These data suggest that in the lungs Pip does affect proliferation of 4T1 cells during metastasis.

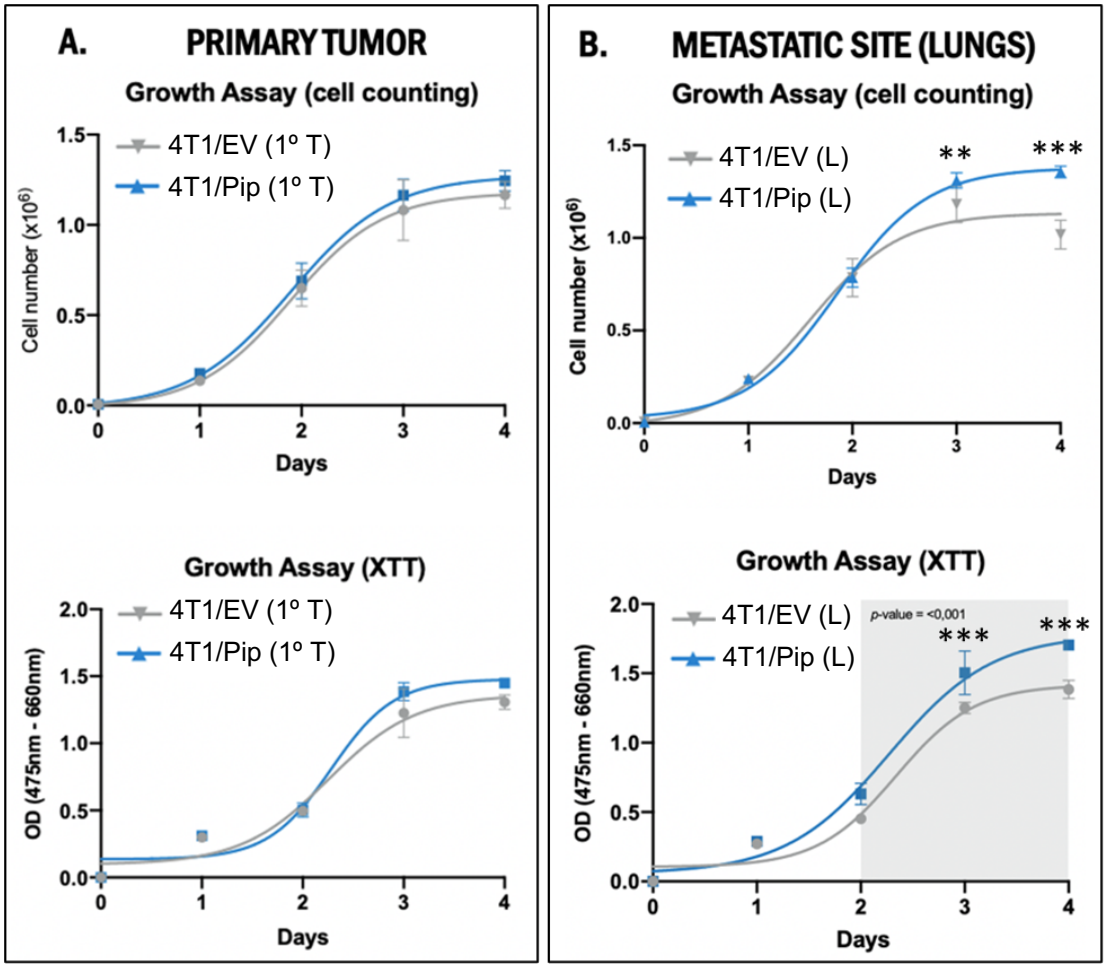

Figure 10 – Enhanced proliferation of *ex vivo Pip* expressing cells isolated from metastatic lung. The proliferation rate of *ex vivo* cells expressing *Pip* (4T1/Pip) derived from the primary tumor was not statistically different from proliferation of control cells (4T1/EV) by both cell counting and a metabolic assay (A). However, proliferation of *ex vivo* cells expressing *Pip* derived from the metastatic lung was significantly higher than proliferation of control cells by both methods (B). Data expressed as mean ± SD. ** $p<0.05$ and *** $p<0.001$, N=4

6.5. *Pip*-expressing 4T1 cells isolated from metastatic lung exhibited enhanced cell migration

To assess the effect of Pip on cell migration, a 3D cell migration assay was used as described in "Material and Methods". Cells isolated from primary tumor displayed no significant difference in cell migration between 4T1 *Pip*-expressing cells and 4T1/EV cells after 6 hours (Figure 11A). However, after 6 hours, 4T1/Pip cells from the metastatic site displayed a higher migration rate when compared to the respective control (4T1/EV); (Figure 11B).

Interestingly, after 20 hours of migration, 4T1/Pip cells derived from the primary tumor continued to show a lower migration rate compared to the control cells, suggesting that *Pip* expression in the primary tumor adversely impacts cell migration (Figure 12A). However, the lung derived 4T1/Pip continued to retain an increased migration rate when compared to control 4T1/EV cells (Figure 12B). These results indicated that in the primary tumor, *Pip* expression delays cell migration, but after metastasis it enhances cell migration.

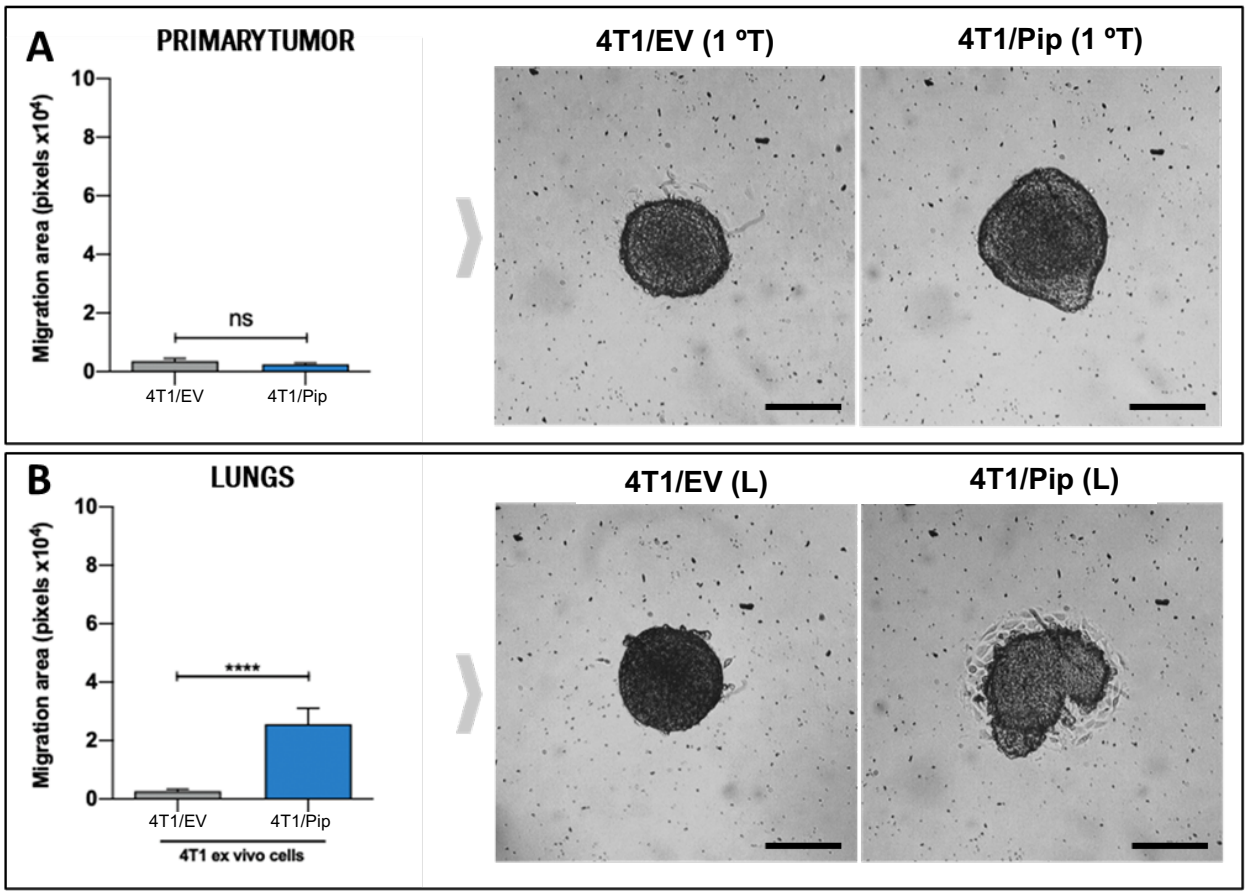

Figure 11 – *Pip* expression in *ex vivo* metastatic lung derived cells enhances cell migration after 6 hours. Migration rates of *ex vivo Pip* expressing cells (4T1/Pip) and control cells (4T1/EV) derived from the primary breast tumor (A) and metastatic lungs (B) were compared after 6 hours. There was no statistical difference in migration, between *Pip* expressing and control cells derived from primary tumor. However, in metastatic lung derived *ex vivo* cells, *Pip* expressing cells show a higher migration rate than control cells. Scale bar, 200 μm. Data expressed as mean $\pm$ SD. **** $p<0.001$, ns = not significant, N=3

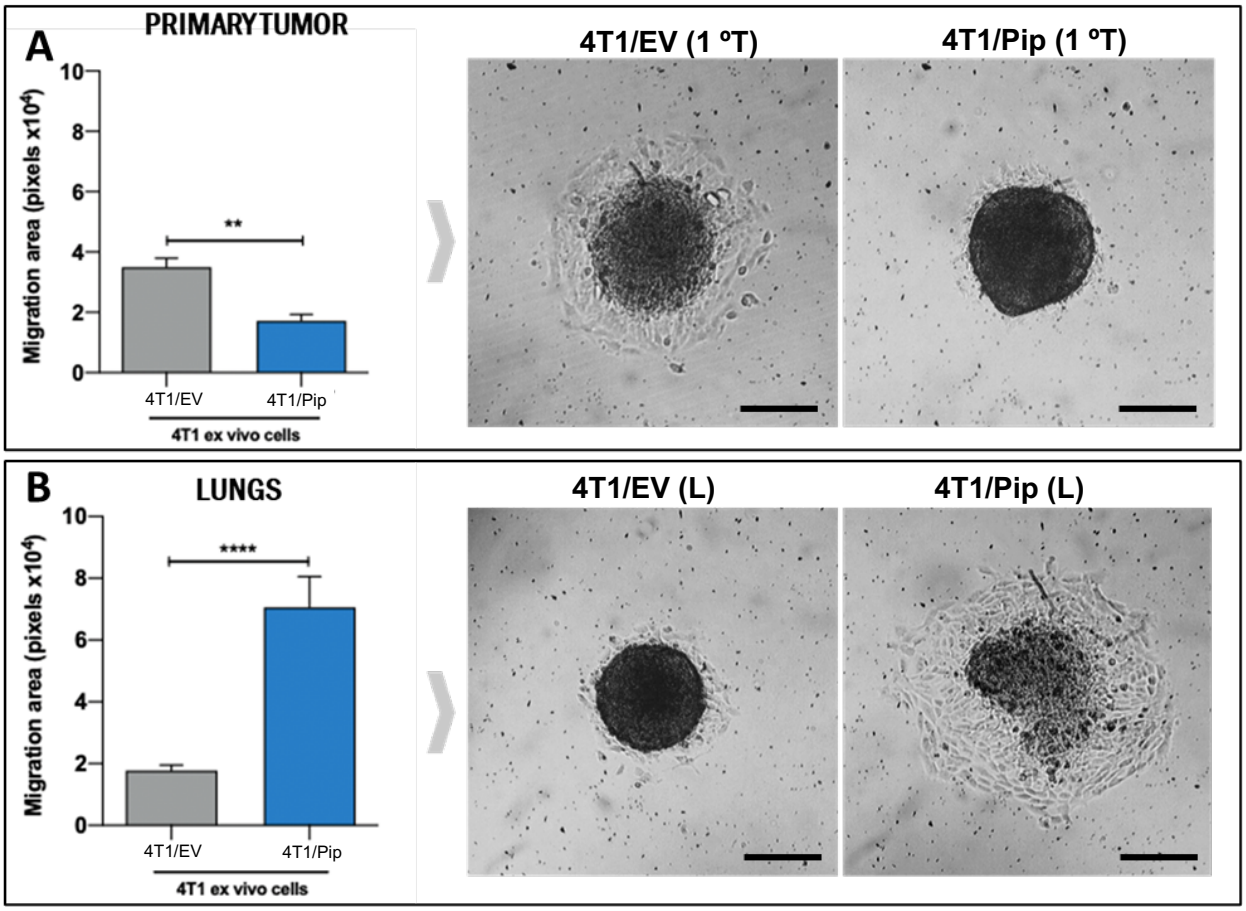

Figure 12 – *Pip* expression in *ex vivo* primary tumor derived cells inhibits migration while in metastatic lung derived cells *Pip* expression enhances cell migration after 20 hours. Migration rates of *ex vivo Pip* expressing cells (4T1/Pip) and control cells (4T1/EV) from primary tumor and metastatic lungs were compared after 20 hours. *Pip* expressing cells derived from primary tumor displayed a lower migration rate than control cells (A). However, in metastatic lung derived *ex vivo* cells, *Pip* expressing cells show a higher migration rate than control cells (B). Scale bar, 200 μm. Data expressed as mean $\pm$ SD. ** $p<0.05$ and *** $p<0.001$, N= 3.

6.6. *Pip*-expressing 4T1 cells isolated from metastatic lung migrate and form secondary colonies

To determine whether Pip-expressing cells are able to generate secondary colonies after they begin to migrate, a 3D migration assay with colony formation was utilized (described in "Material and Methods"). As shown in Figure 13A, virtually no significant difference in colony numbers between 4T1/Pip and the 4T1/EV cells from primary tumor was observed. However, Figure 13B, shows that lung derived 4T1/Pip cells established more distal colonies when compared to the control counterparts (4T1/EV). These results show that *Pip* expression in 4T1 cells in lung enhances secondary colony formation.

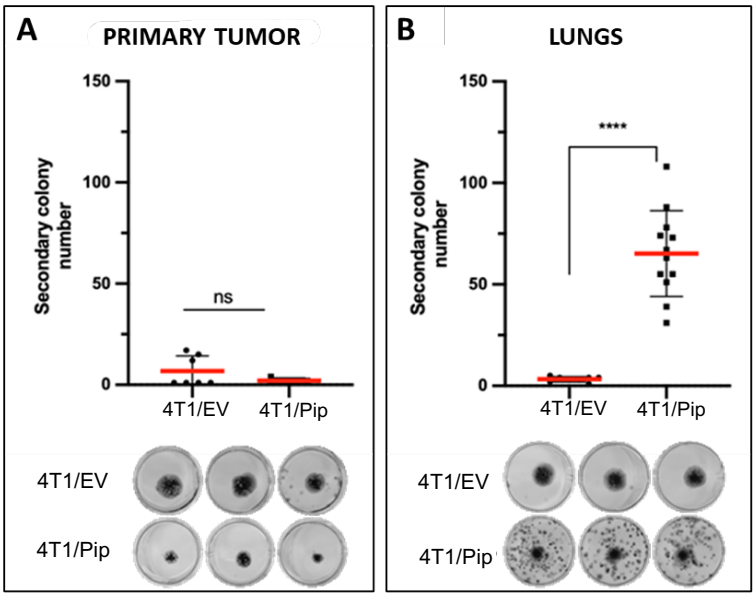

Figure 13 – *Pip* expression in *ex vivo* metastatic lung derived cells enhances colony formation. Colony forming ability of *ex vivo Pip* expressing cells (4T1/Pip) and control cells (4T1/EV) derived from both primary tumor (A) and metastatic lungs (B) were compared using a colony formation assay. Only *Pip* expressing cells derived from lung displayed a higher colony formation ability compared to control cells. Data expressed as mean ± SD, **** $p<0.001$, ns = not significant, N=3.

6.7. *Pip* expression induces EMT in 4T1 cells isolated from the lungs

To gain insight into why 4T1 *Pip*-expressing cells isolated from lungs displayed a change in morphology following metastasis, Western Blot analysis was used to determine the levels of the epithelial proteins (ZO-1 and E-Cadherin) as well as the mesenchymal protein (Vimentin) known markers of EMT. In addition, expression of transcription factors associated with the activation of the EMT process, Twist, Snail and Slug were evaluated by RT-qPCR.

4T1/Pip cells isolated from lungs show a significant decrease of ZO-1 and E-Cadherin proteins and an increase in vimentin protein when compared to the 4T1/EV control. This indicates that *Pip*-expressing cells isolated from metastatic lung may be undergoing the EMT process. From the primary tumor, there was no difference between the levels of ZO-1 and E-Cadherin between 4T1/Pip and control, however Vimentin was significantly lower in 4T1/Pip (Figure 14A).

The results of the qPCR studies are shown in Figure 14B, in which Vimentin, Twist and Snail expression were significantly up regulated in 4T1/Pip cells from the lungs when compared to control cells. These results indicate that changes in morphology in 4T1 *Pip*-expressing cells from the metastatic site are mostly likely due to activation of the EMT process.

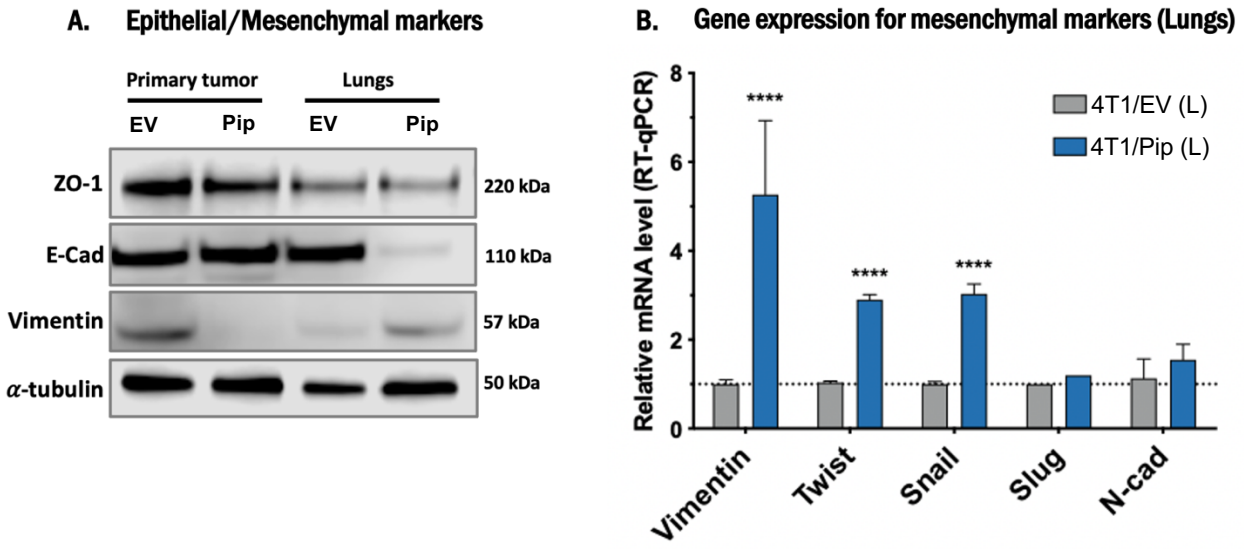

Figure 14 – *Pip* expressing *ex vivo* metastatic lung derived cells undergo EMT. EMT associated proteins were examined by Western Blotting (A) and RT-qPCR (B). *Pip* expressing cells derived from lung show a decrease in the epithelial markers (ZO-1 and E-Cadherin) and increase in the mesenchymal protein vimentin (A). An upregulation of genes expressing mesenchymal markers is observed in *Pip* expressing cells derived from lung (vimentin, twist, and snail). Data is expressed as mean $\pm$ SD, ****$p<0.001$.

6.8. *Pip* expression in 4T1 cell isolated from the lungs increases ERK1/2 phosphorylation in the presence of fibronectin

Fibronectin is one of the major components of the ECM. Because of its RGD sequence it can bind and activate the α5β1 integrin, which in turn triggers the activation of intracellular pathways related to cell migration, proliferation, and survival, mainly mediated by ERK1/2.

To test the hypothesis that fibronectin fragments produced by Pip aspartic protease activity are responsible for ERK1/2 activation, *Pip* expressing 4T1 cells and controls from both primary tumor and lungs were grown on a fibronectin-coated surface and the levels of ERK1/2 phosphorylation determined by Western blot analysis.

We observed that in the presence of fibronectin, 4T1 *Pip*-expressing cells derived from the primary tumor, show a lower level of ERK1/2 phosphorylation than 4T1/EV control cells. However, the lung-derived *Pip*-expressing 4T1 cells show a significant increase in ERK1/2 phosphorylation ratio in the presence of fibronectin when compared to the 4T1/EV cells (control). These results indicate that *Pip* expression facilitates activation of ERK1/2 in 4T1 cells isolated from the lungs, but not from the primary tumor (Figure 15).

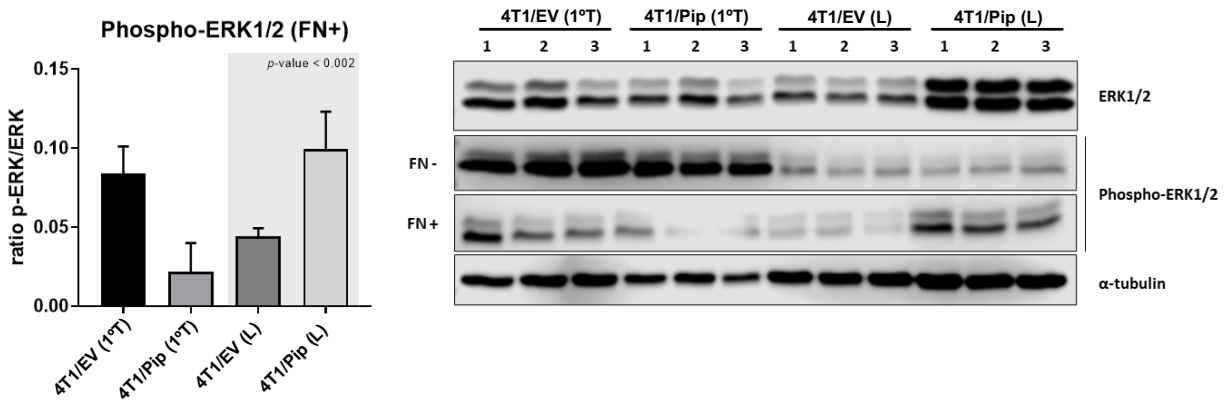

Figure 15 – *Pip* expression in *ex vivo* metastatic lung derived cells increases p-ERK1/2 levels in the presence of fibronectin. The level of p-ERK1/2 was determined in *ex vivo Pip* expressing cells (4T1/Pip) and control cells (4T1/EV) derived from primary tumor and metastatic lungs that were grown either on fibronectin coated plates (FN +) or in the absence of fibronectin (FN -) as described in "Methods". Western blot analysis shows an increase in the ratio of phosphorylated ERK1/2 to total ERK1/2 in PIP expressing cells from lung when grown in the presence of fibronectin. Data is expressed as mean ± SD, ****p<0.001.

6.9. ERK1/2 phosphorylation is associated with increased cell proliferation

To determine whether the increase in ERK1/2 phosphorylation impacts the cellular behaviour of 4T1/Pip cells isolated from lung, a cell proliferation assay was carried out using coated and un-coated fibronectin plates. Figure 16A shows that in the presence of fibronectin, the 4T1 *Pip*-expressing cells from lungs displayed a higher proliferation rate when compared to similar cells cultured in a non-coated fibronectin plate (control). However, figure 16B shows that in non-*Pip* expressing cells from lungs (4T1/EV) the presence of fibronectin makes no difference in cell proliferation. These results suggest that in 4T1 cells isolated from metastatic site, *Pip* expression increases cell proliferation through a pathway involving the activation of ERK1/2.

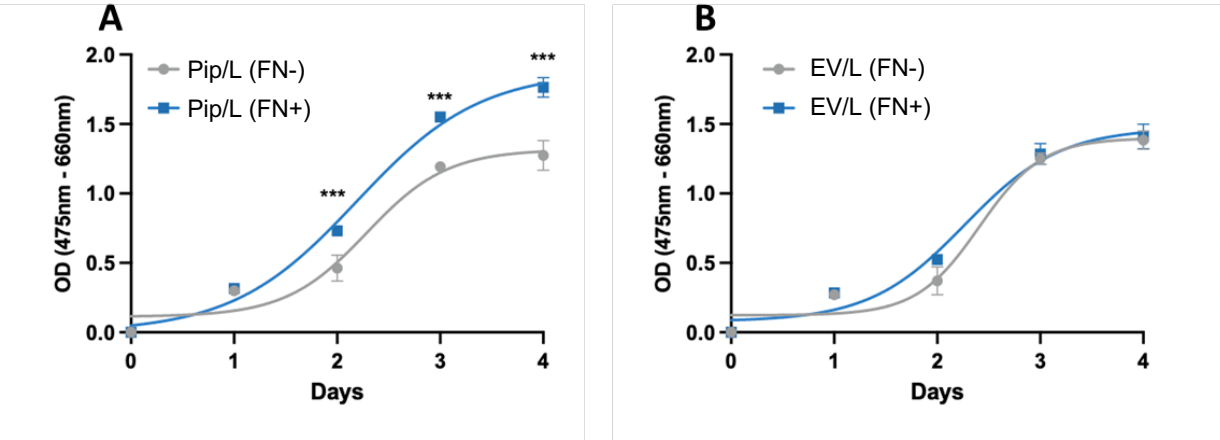

Figure 16 – In *ex vivo* metastatic lung derived cells, *Pip* expression increases cell proliferation in the presence of fibronectin. *Pip* expressing cells (4T1/Pip) and control cells (4T1/EV) cells derived from metastatic lungs were grown either on fibronectin coated plates (FN +) or in the absence of fibronectin (FN -) and the proliferation rate determined as described in "Methods". *Pip* expressing *ex vivo* metastatic lung derived cells show increased proliferation in the presence of fibronectin (A). Control cells from lung show no change in proliferation in the presence of fibronectin (B). Data expressed as mean ± SD, ***p<0.001, N=4.

7. DISCUSSION

The role of PIP in BC metastasis has not yet been fully elucidated. Current studies from our research group suggest a double-edged effect for PIP during breast tumor progression (Edechi et al., 2021). The aim of this study was to assess the role of PIP in TNBC metastasis using a transplantable mouse model of BC generated in our laboratory and *ex vivo* cultures of 4T1 *Pip*-expressing cells isolated from both the primary tumor as well as the metastatic lung.

Pip-expressing 4T1 cells (4T1/Pip) as well as respective control 4T1 non-*Pip* expressing cells (4T1/EV) were isolated from a BALB/C mouse bearing 4T1 tumors 3 weeks following orthotopic injections into the 4th mammary fat pad. Western blot analysis was used to evaluate whether Pip levels would remain the same between the 4T1 cells isolated from the primary tumor versus the 4T1 cells isolated from the lung metastatic site. The levels of Pip protein were found to be similar in the 4T1 cells isolated from both sites, indicating that during the metastatic process, the level of Pip secretion by the cells remained virtually the same. Thus, any differences observed between the cells derived from primary tumor and the cells from metastatic site could not be attributed to differences in Pip protein levels. However, the unchanged expression of *Pip* during tumor metastasis could be a result of its inducible expression by lentivirus transduction, as the insertion of *Pip* coding sequence into the genomic DNA of 4T1 cells was not locus specific. As a result, *Pip* expression is not modulated by its natural inducers. To gain further insight into how *Pip* expression facilitates 4T1 TNBC metastasis, a qPCR array analysis revealed several differentially expressed metastatic genes in the *Pip*-expressing cells versus control (4T1/EV) cells isolated from lung. Most notably, a group of metalloproteinases (MMP-2, -3, -9, -10, -11, -13) and fibronectin (FN1) genes were significantly up-regulated. Up-regulation of MMPs have been previously reported during TNBC metastasis as they can digest the majority of ECM components,

which facilitate ECM remodeling leading to intravasation and extravasation of tumor cells by releasing several cytokines and growth factors required for tumor progression (Mehner et al., 2014; Yang et al., 2014; Shi et al., 2016). For example, MMPs can indirectly modulate TGF-β bioactivity by cleaving the ECM component, latent TGF-β-binding protein 1 (LTBP-1), thereby solubilizing ECM-bound TGF-β (Kessenbrock et al., 2010). Furthermore, high levels of FN1 gene expression have been negatively correlated to an advanced stage of BC with poor clinical outcome (Chen et al., 2021; Helleman et al., 2008). Furthermore, it has been suggested that the increase of FN1 expression may be associated with lung tumor survival, growth, and resistance to therapy (Han et al., 2006). It is thus conceivable that Pip may upregulate the expression of these genes by regulating pathways resulting in the activation of these genes.

Given that *Pip* expression up-regulated genes involved in the metastatic process, the STRING database coupled with gene ontology was used to identify specific biological processes associated with the up-regulated genes. The enriched pathways observed were associated with "extracellular matrix organization", "positive regulation of cell migration", "extracellular matrix disassembly", "regulation of cell proliferation" and "angiogenesis". The pathways identified are common processes found in several types of cancer and are major steps required for tumor progression and metastasis.

The biological pathways were verified using experimental approaches to evaluate proliferation, migration, and colony formation. Cell counting and XTT assay were employed as complementary methods to evaluate the effect of *Pip* expression on the proliferation of 4T1 cells from primary tumor and lungs.

Results obtained from both assay show that *Pip* expression in the primary tumor does not influence 4T1 cell proliferation when compared to control. However, in the 4T1 cells isolated from

the lungs, *Pip* expression enhanced proliferation. The non-proliferative effect of Pip in the cells isolated from the primary tumor agrees with previous studies conducted showing that inducing *Pip* expression in mouse BC cells did not influence cell proliferation in an *in vitro* model (Edechi et al., 2021). However, studies using a human BC cell line showed that PIP protein induces a mitogenic response (Cassoni et al., 1995; Baniwal et al., 2013). The first study by Edechi et al. (2021) used the 4T1 mouse cell line originally isolated from primary tumor in a mammary gland of a BALB/C mouse while the studies conducted by Cassion et al. and Baniwal used human BC cell lines (MDA-MB-231, T-47D and MCF-7) originally isolated from the pleural effusion of BC patients with metastatic disease. The differences between the mouse and human studies strongly suggest that a component of the tumor microenvironment influences the effect of PIP, and that during metastasis changes that occur in the BC cells may favor PIP function or that the "soil" selects for a pre-existing clonal phenotype displaying advantages for growth in this niche.

BC cells, like many other cancer cell types, are known to migrate from the primary tumor location to secondary tissues. Acquisition of the ability to migrate is an important step in cancer progression. To study the effect of *Pip* expression on the migratory ability of 4T1 cells isolated from both the primary tumor site and lung were investigated using a 3D cell spheroid assay as well as a colony formation assay. The use of two complementary approaches strengthens the reliability and validity of the results. In both assays, *Pip*-expressing 4T1 cells isolated from the metastatic site had a higher migration and colony formation capability. Not surprisingly, the *Pip*-expressing cells isolated from primary tumor showed both lower migration and colony formation. Previous studies by others also showed that PIP is necessary to regulate cell migration, cytoskeleton dynamics, cell adhesion and invasion of human BC cell lines (Zheng et al., 2013). The enhanced cell migration observed in our current study and the ability to form secondary colonies also agrees

with previous studies that found PIP expression regulates phosphorylation of specific Receptor Tyrosine Kinases (RTKs) and downstream signaling pathways involving the AKT, ERK1/2, JNK1 and cMYC (Baniwal et al., 2013). These pathways have been extensively described as key factors that promote BC tumor progression due to their ability to inhibit apoptosis and promote cell cycle progression and cell motility. These results reinforce the double-edge theory of PIP as we have previously observed: in the primary tumor Pip works as a protective protein by delaying tumor onset, while in the metastatic site it promotes secondary tumor establishment and metastatic progression (Edechi et al., 2021).

Interestingly, when the 4T1 cells were initially isolated from the primary breast tumor and metastatic lung, differences in morphology were observed. Evaluation of cell morphology showed that *Pip*-expressing 4T1 cells isolated from lung underwent morphological changes during the metastasis process. During cancer progression, only specific tumor phenotypes that result from molecular and morphological alterations can pass through the walls of blood or lymphatic vessels and are therefore able to freely circulate in the bloodstream to reach other tissues in the body. Tumor cells must alter the expression level of some proteins in order to survive outside of the tumor microenvironment and reach distant sites. Evaluation of cell morphology following phalloidin staining of 4T1/Pip from lung suggested these cells had undergone epithelial-to-mesenchymal transition (EMT). EMT is usually associated with the loss of cell apicobasal polarity and cell-cell adhesion and the acquisition of migratory and invasive properties, along with a switch of epithelial markers to mesenchymal markers. Additionally, *Pip*-expressing cells isolated from the lungs also displayed a compact nucleus and reduced cytoplasm. These observations are strongly correlated with the metastatic process as it has been extensively reported that chromatin compaction favors structural modifications to the nucleus which are required steps to metastatic

cell invasion through small gaps in the extracellular matrix (Gauthier et al., 2022; Navarro-Lerida et al., 2015). Moreover, the presence of micronuclei in 4T1/Pip cells from primary tumor was observed. These structures are small DNA-containing nuclear structures that are spatially isolated from the main nucleus. The formation of micronuclei is frequent associated with genomic instability and is found in pathologies, including cancer. In fact, recent studies showed that micronuclei formation is directly associated with altered gene-expression profile, and increased BC metastasis in xenograft model and altered gene-expression profile (Haimovici et al., 2022). The presence of micronuclei in the 4T1/Pip from primary tumor could indicate an increase of genomic instability and cell clonal evolution, commonly observed in aggressive tumors (Kwon et al., 2020).

To confirm that *Pip* expression facilitated EMT in 4T1 cells, the expression of epithelial and mesenchymal markers was evaluated by Western blot and qPCR. It was found in the 4T1/Pip cells isolated from lungs that ZO-1 and E-Cadherin (epithelial proteins associated with tight and adheren junctions, respectively) were downregulated, while Vimentin (intermediate filament, highly expressed in mesenchymal cells) was up-regulated. The loss of cell to cell contact in the 4T1/Pip cells from lungs may be associated with the lower levels of the ZO-1 and E-Cadherin as these proteins are essential to maintain tight junctions and adhesion function integrity. The loss of tight junction proteins in metastatic BC cells is frequently reported and is suggested as one of the main mechanisms that facilitates metastasis of tumors originating from epithelial tissues. Furthermore, transcription factors Twist and Snail, key positive regulators of EMT process, were up-regulated as shown by qPCR. The increase of expression of Twist and Snail explains the decreased levels of E-Cadherin and ZO-1, as these transcription factors inhibit the expression of several proteins associated with tight junctions and adhesion junctions (Masuda et al., 2010;

Kurrey et al., 2005). Additionally, Vimentin is known to promote cell migration by enhancing contact-dependent cell stiffening (Battaglia et al., 2018). Thus, the high levels of Vimentin found in the 4T1/EV from primary tumor and 4T1/Pip from lungs by Western blot could explain the high motility rate found in these cells using the migration assay. Collectively, these results show an endothelial to mesenchymal transition in 4T1 *Pip* expressing cells that may facilitate metastasis to the lung. The activation of the EMT process coincides with an increase of MMPs expression in the *Pip* expressing 4T1 cells from the lungs. Up-regulation of MMPs during EMT result in ECM remodeling, which ultimately facilitates cell extravasation.

Fibronectin (FN) is a component of the extracellular matrix, and its role in tumorigenesis and malignant progression is highly controversial (Lin et al., 2019). Expression of FN in tumor cells is thought to play a role in tumor suppression by preventing tumor transformation and early progression (Plath et al., 2000; Yi and Ruoslahti, 2001). However, abundant evidence reveals that FN is often associated with later stages of cancer metastasis and when expressed in tumor cells is associated with a poor prognosis (Fernandez-Garcia et al., 2014; Malik et al., 2010; Humphries et al., 1989). The enzymatic cleavage of fibronectin by the aspartyl protease activity of the PIP protein itself can release fragments containing a RGD motif that can more easily bind to membrane proteins, specifically the $\alpha 5\beta 1$ integrin, known as the "fibronectin receptor". The activation of integrin-$\beta 1$ promotes cell adhesion and invasion (Schaffner et al., 2013) as well as inducing some signaling pathways such as MAPK/ERK that are involved in cell proliferation, migration and survival (Jin et al., 2011; Morozevich et al., 2009).

To investigate whether the fibronectin-degrading ability of PIP activates the MAPK/ERK pathway, *Pip*-expressing 4T1 cells isolated from primary tumor and a metastatic site in the lungs were cultured in the presence of fibronectin. When *Pip*-expressing cells isolated from the primary

tumor were cultured with fibronectin the level of activated ERK1/2 was less than that seen with *Pip* expressing cells isolated from the metastatic site. These observations support the idea that following metastasis, a subpopulation of BC cells selected by the lung microenvironment, can become more reactive to fibronectin facilitating ERK1/2 activation.

Interestingly, the increase of ERK1/2 phosphorylation in *Pip*-expressing cells from a metastatic site might indicate a mechanism for PIP driving BC metastasis. In fact, previous studies using a human molecular apocrine tumor (MDA-MB-453) also demonstrated that the fibronectin-degrading ability of PIP was able to activate the integrin-linked kinase 1 (ILK1), which binds to the activated integrin-β1 and mediate downstream signaling effects such as the activation of MAPK/ERK and PI3K/AKT. Furthermore, in several subtypes of BC it has been demonstrated that activation of ERK1/2 can lead to an augmentation of transcription factors such as, Slug, Snail and Twist that mediates the activation of the EMT process. Interestingly, both 4T1 *Pip*-expressing cells and control from primary tumor showed a higher ERK1/2 phosphorylation in the absence of fibronectin. This observation could be explained by the fact that ERK1/2 could be activated in the primary tumor by other mechanisms such aberrant expression/ or activation of receptors that can trigger ERK1/2 pathway such as members of receptor tyrosine kinase or fibroblast growth factor receptors (FGFR). Furthermore, recent studies found that selective inhibition of FGFR resulted in a decreased activation of ERK1/2 as well as PI3K/AKT in 4T1 cells, leading to the activation of apoptosis (Issa et al., 2013). The high levels of ERK1/2 in the primary tumor cells can also be an adaptative response to the selective pressures that the cells were under in the primary tumor environment.

The phosphorylation of ERK1/2 and the activation of its downstream pathways is strongly associated with increase of cell mitotic potential. To investigate if fibronectin fragments generated

by Pip enzymatic degradation could impact the mitotic potential of *Pip*-expressing 4T1 cells isolated from the metastatic site, proliferation assays in the presence or absence of fibronectin treatment were performed. In the presence of fibronectin, *Pip*-expressing cells from metastatic site showed an increase in cell proliferation when compared to the cells cultured in the absence of fibronectin. The fibronectin effect on proliferation appears to be dependent on *Pip* expression as there is no difference between proliferation rate in the non-*Pip* expressing cells either with or without fibronectin treatment.

This collective data are indicative that *Pip* plays a role in BC metastasis through the indirect activation of the fibronectin receptor ($\alpha5\beta1$ integrin), which leads to the activation of downstream pathways that ultimately facilitate tumor progression and metastasis.

8. SUMMARY AND CONCLUSIONS

In this study, the role of PIP in BC metastasis was assessed using *ex vivo* cultures of 4T1 *Pip*-expressing cells isolated from both the primary and metastatic site tumors using a transplantable mouse model of TNBC. Gene analysis of the *ex vivo* cells revealed that the expression of *Pip* during the metastatic process induces the activation of several biological processes that favor tumor establishment and progression.

Characterization of the *ex vivo* BC cells grown in culture showed that following BC metastasis, Pip levels remained the same in the cells from primary tumor as well as the cells from the metastatic site. Further characterization showed that *Pip*-expressing cells isolated from metastatic site displayed higher proliferation when compared to controls. In the primary tumor, *Pip* expression in 4T1 cells seemed to reduce cell migration but, 4T1/*Pip* expressing cells from the lung exhibited a greater migration ability when compared to the controls. In addition to the enhanced migration observed, 4T1/*Pip* cells isolated from lung formed more cell colonies in the tissue culture plates when compared to the non-*Pip* expressing cells.

Morphological analysis revealed that during BC metastasis to the lungs, *Pip* expression induced EMT process in the cells, as the 4T1 cells lost their epithelial morphology becoming more mesenchymal-like. These finding agreed with results observed by Western Blot analysis and qPCR which show a reduction in epithelial proteins (ZO-1 and E-Cadherin) and increase in the mesenchymal markers (Vimentin, Twist and Snail).

Pip was also found to indirectly activate the ERK1/2 signaling pathway through its ability to degrade fibronectin resulting in increase of proliferation.

Collectively, these data suggest that Pip plays a role in BC metastasis by activating important pathways that ultimately facilitate tumor invasion and establishment in secondary sites.

Most importantly, it supports the possibility that Pip function is determined by the surrounding tumor microenvironment.

9. LIMITATIONS OF THIS STUDY

1. A major limitation of this study is that results obtained from mice *ex vivo* cell culture models may not completely reflect what occurs in humans *in vivo*, due to species differences.
2. Another limitation is that *ex vivo* cultures of isolated BC cells, even though tissue derived, lack the *in vivo* tumor microenvironment where the tumor cells are surrounded by host stroma cells with which they constantly communicate and interact.

10. SIGNIFICANCE

This study provides important preclinical data that shows Pip to be an important regulator of BC tumor metastasis. In addition to the data demonstrating that Pip can differently modulate BC cell behaviour in the primary tumor and in the metastatic site in lung, we have further shown that Pip may enhance BC cells aggressiveness by indirectly activating the ERK1/2 pathway though fibronectin cleavage. This important observation could have potential applications for the management of BC patients. Furthermore, observations generated through these studies suggest that Pip enhances BC metastasis by its aspartyl protease activity on the extracellular matrix. Thus, the use of molecules that block the aspartyl protease activity may provide alternative treatment for BC patients with high levels of PIP. As well, careful monitoring of the levels of PIP in BC patients may be a predictive factor to determine metastatic potential.

11. FUTURE DIRECTIONS

Metastasis is the major cause of mortality in BC patients and the precise mechanisms by which *Pip* expression promotes metastasis is yet not fully understood. I have shown in this study that Pip can differently modulate 4T1 cell behaviour depending on the tissue microenvironment. We now have to evaluate if this effect is also observed with different BC cell lines. For this, human TNBC cells lines such as HCC1937 and HCC1143 that express *PIP* could be used to develop xenograft models to facilitate the study of PIP function during metastasis.

Since PIP can degrade fibronectin and we found that in the presence of fibronectin 4T1/Pip cells had an increase in ERK1/2 phosphorylation, further studies to confirm that fibronectin fragments are activating integrins are required. For that, 4T1/Pip cells could be cultured on fibronectin-coated plated and then immunoprecipitation (IP) of the integrin α5 subunit following immunodetection of fibronectin could be performed. If this hypothesis is correct, we expect to detect a positive band for fibronectin following IP procedures, indicating that the fibronectin fragments are indeed activating the integrins. Additionally, to prove causality between fibronectin fragments activating ERK1/2 phosphorylation, 4T1 *Pip*-expressing cells can be cultured with or without fibronectin and block protein phosphorylation in order to evaluate whether fibronectin is required to activate ERK1/2.

It is also possible that during metastasis 4T1 cells have upregulated the levels of α5β1 integrins, which facilitates its activation by fibronectin fragments. To explore that possibility, Western blot and qPCR assays can be used to evaluate the integrin levels in the 4T1/Pip cells from both primary tumor and metastatic site in the lungs.

Since the main source of fibronectin in the tumor microenvironment is secreted by fibroblast cells, it is possible that fibronectin fragments may also modulate host fibroblast that in

turn can secret factors that further facilitate tumor progression. To investigate the in-depth contribution of fibroblasts, a 3D co-culture with 4T1/*Pip* expressing cells will be performed. We intend to characterize 4T1 cell behaviour in presence of fibroblasts using mRNA analysis to determine whether co-culture with fibroblasts can impact the expression of genes important to metastasis.

Finally, to evaluate the interactions of Pip protein, IP coupled with mass spectrometry can be performed to identify proteins that are interacting with Pip and evaluate whether these interactions are different between the primary tumor site and metastatic site in the lungs. This will also provide an opportunity to identify new protein candidates that may be facilitating prolactin inducible protein function during BC metastasis.

12. REFERENCES

1. Breast cancer statistics [Internet]. World Cancer Research Fund. 2018 [cited 2022 Sept 5]. Available from: https://www.wcrf.org/dietandcancer/cancer-trends/breast-cancer-statistic
2. Sung, H., Ferlay, J., Siegel, R. L., Laversanne, M., Soerjomataram, I., Jemal, A., & Bray, F. (2021). Global cancer statistics 2020: GLOBOCAN estimates of incidence and mortality worldwide for 36 cancers in 185 countries. CA: a cancer journal for clinicians, 71(3), 209-249.
3. Huang, J., Chan, P. S., Lok, V., Chen, X., Ding, H., Jin, Y., ... & Wong, M. C. (2021). Global incidence and mortality of breast cancer: a trend analysis. *Aging (Albany NY)*, *13*(4), 5748.
4. Sharma, R. (2019). Breast cancer incidence, mortality and mortality-to-incidence ratio (MIR) are associated with human development, 1990–2016: evidence from Global Burden of Disease Study 2016. *Breast Cancer*, *26*(4), 428-445.
5. Fitzmaurice, C., Akinyemiju, T. F., Al Lami, F. H., Alam, T., Alizadeh-Navaei, R., Allen, C., ... & Yonemoto, N. (2018). Global, regional, and national cancer incidence, mortality, years of life lost, years lived with disability, and disability-adjusted life-years for 29 cancer groups, 1990 to 2016: a systematic analysis for the global burden of disease study. *JAMA oncology*, *4*(11), 1553-1568.
6. Breast Cancer Statistics – Canadian Cancer Society [internet] www.cancer.ca. [cited June 2022] Available from: https://cancer.ca/en/cancer-information/cancer-types/breast/statistics.
7. Canadian Cancer Statistics 2022 – Canadian Cancer Society [internet] www.cancer.ca. [cited June 2022] Available from: Canadian Cancer Statistics | Canadian Cancer Society

8. Brenner, D. R., Weir, H. K., Demers, A. A., Ellison, L. F., Louzado, C., Shaw, A., ... & Smith, L. M. (2020). Projected estimates of cancer in Canada in 2020. *Cmaj*, *192*(9), E199-E205.

9. Howlader, N., Cronin, K. A., Kurian, A. W., & Andridge, R. (2018). Differences in breast cancer survival by molecular subtypes in the United States. *Cancer Epidemiology, Biomarkers & Prevention*, *27*(6), 619-626.

10. Azamjah, N., Soltan-Zadeh, Y., & Zayeri, F. (2019). Global trend of breast cancer mortality rate: a 25-year study. *Asian Pacific journal of cancer prevention: APJCP*, *20*(7), 2015.

11. Waks, A. G., & Winer, E. P. (2019). Breast cancer treatment: a review. Jama, 321(3), 288-300.

12. Tsang, J., & Tse, G. M. (2020). Molecular classification of breast cancer. *Advances in anatomic pathology*, *27*(1), 27-35.

13. Vuong, D., Simpson, P. T., Green, B., Cummings, M. C., & Lakhani, S. R. (2014). Molecular classification of breast cancer. *Virchows Archiv*, *465*(1), 1-14.

14. Pusztai, L., Mazouni, C., Anderson, K., Wu, Y., & Symmans, W. F. (2006). Molecular classification of breast cancer: limitations and potential. *The oncologist*, *11*(8), 868-877.

15. Zepeda-Castilla, E. J., Recinos-Money, E., Cuéllar-Hubbe, M., Robles-Vidal, C. D., & Maafs-Molina, E. (2008). Molecular classification of breast cancer. *Cirugia y cirujanos*, *76*(1), 87-93.

16. Andre, F., & Pusztai, L. (2006). Molecular classification of breast cancer: implications for selection of adjuvant chemotherapy. *Nature clinical practice Oncology*, *3*(11), 621-632.

17. Bianchini, G., Balko, J. M., Mayer, I. A., Sanders, M. E., & Gianni, L. (2016). Triple-negative breast cancer: challenges and opportunities of a heterogeneous disease. *Nature reviews Clinical oncology*, *13*(11), 674-690.

18. Wolff, A. C., Hammond, M. E. H., Hicks, D. G., Dowsett, M., McShane, L. M., Allison, K. H., ... & Hayes, D. F. (2014). Recommendations for human epidermal growth factor receptor 2 testing in breast cancer: American Society of Clinical Oncology/College of American Pathologists clinical practice guideline update. *Archives of Pathology and Laboratory Medicine*, *138*(2), 241-256.

19. Medina, M. A., Oza, G., Sharma, A., Arriaga, L. G., Hernández Hernández, J. M., Rotello, V. M., & Ramirez, J. T. (2020). Triple-negative breast cancer: a review of conventional and advanced therapeutic strategies. *International journal of environmental research and public health*, *17*(6), 2078.

20. Lehmann, B. D., Jovanović, B., Chen, X. I., Estrada, M. V., Johnson, K. N., Shyr, Y., ... & Pietenpol, J. A. (2016). Refinement of triple-negative breast cancer molecular subtypes: implications for neoadjuvant chemotherapy selection. *PloS one*, *11*(6), e0157368.

21. Yam, C., Mani, S. A., & Moulder, S. L. (2017). Targeting the molecular subtypes of triple negative breast cancer: understanding the diversity to progress the field. *The oncologist*, *22*(9), 1086-1093.

22. Hudis, C. A., & Gianni, L. (2011). Triple-negative breast cancer: an unmet medical need. *The oncologist*, *16*(S1), 1-11.

23. Khan, W., Ashfaq, U. A., Aslam, S., Saif, S., Aslam, T., Tusleem, K., ... & ul Qamar, M. T. (2017). Anticancer screening of medicinal plant phytochemicals against Cyclin-Dependent Kinase-2 (CDK2): An in-silico approach. *Advancements in Life Sciences*, *4*(4), 113-119.

24. Tsai, J., Bertoni, D., Hernandez-Boussard, T., Telli, M. L., & Wapnir, I. L. (2016). Lymph node ratio analysis after neoadjuvant chemotherapy is prognostic in hormone receptor-positive and triple-negative breast cancer. *Annals of Surgical Oncology*, *23*(10), 3310-3316.

25. Singh, S., Numan, A., Agrawal, N., Tambuwala, M. M., Singh, V., & Kesharwani, P. (2020). Role of immune checkpoint inhibitors in the revolutionization of advanced melanoma care. *International Immunopharmacology*, *83*, 106417.

26. Dent, R., Trudeau, M., Pritchard, K. I., Hanna, W. M., Kahn, H. K., Sawka, C. A., ... & Narod, S. A. (2007). Triple-negative breast cancer: clinical features and patterns of recurrence. *Clinical cancer research*, *13*(15), 4429-4434.

27. Dietze, E. C., Sistrunk, C., Miranda-Carboni, G., O'regan, R., & Seewaldt, V. L. (2015). Triple-negative breast cancer in African-American women: disparities versus biology. *Nature Reviews Cancer*, *15*(4), 248-254.

28. SUGITA, Bruna et al. Differentially expressed miRNAs in triple negative breast cancer between African-American and non-Hispanic white women. **Oncotarget**, v. 7, n. 48, p. 79274, 2016.

29. Kohler, B. A., Sherman, R. L., Howlader, N., Jemal, A., Ryerson, A. B., Henry, K. A., ... & Penberthy, L. (2015). Annual report to the nation on the status of cancer, 1975-2011, featuring incidence of breast cancer subtypes by race/ethnicity, poverty, and state. *Journal of the National Cancer Institute*, *107*(6), djv048.

30. Paget, S. (1889). The distribution of secondary growths in cancer of the breast. *The Lancet*, *133*(3421), 571-573.

31. Lambert, A. W., Pattabiraman, D. R., & Weinberg, R. A. (2017). Emerging biological principles of metastasis. *Cell*, *168*(4), 670-691.

32. Kotiyal, S., & Bhattacharya, S. (2014). Breast cancer stem cells, EMT and therapeutic targets. *Biochemical and biophysical research communications*, *453*(1), 112-116.

33. Bill, R., & Christofori, G. (2015). The relevance of EMT in breast cancer metastasis: Correlation or causality?. *FEBS letters*, *589*(14), 1577-1587.

34. Derynck, R., & Weinberg, R. A. (2019). EMT and cancer: more than meets the eye. *Developmental cell*, *49*(3), 313-316.

35. Zhang, Y., & Weinberg, R. A. (2018). Epithelial-to-mesenchymal transition in cancer: complexity and opportunities. *Frontiers of medicine*, *12*(4), 361-373.

36. Pearson, G. W. (2019). Control of invasion by epithelial-to-mesenchymal transition programs during metastasis. *Journal of clinical medicine*, *8*(5), 646.

37. Sinha, D., Saha, P., Samanta, A., & Bishayee, A. (2020). Emerging concepts of hybrid epithelial-to-mesenchymal transition in cancer progression. *Biomolecules*, *10*(11), 1561.

38. Bornes, L., Belthier, G., & van Rheenen, J. (2021). Epithelial-to-mesenchymal transition in the light of plasticity and hybrid E/M states. *Journal of Clinical Medicine*, *10*(11), 2403.

39. Liao, T. T., & Yang, M. H. (2020). Hybrid epithelial/mesenchymal state in cancer metastasis: clinical significance and regulatory mechanisms. *Cells*, *9*(3), 623.

40. Chen, Y., Tan, W., & Wang, C. (2018). Tumor-associated macrophage-derived cytokines enhance cancer stem-like characteristics through epithelial–mesenchymal transition. *OncoTargets and therapy*, *11*, 3817.

41. Vakili-Ghartavol, R., Mombeiny, R., Salmaninejad, A., Sorkhabadi, S. M. R., Faridi-Majidi, R., Jaafari, M. R., & Mirzaei, H. (2018). Tumor-associated macrophages and epithelial–mesenchymal transition in cancer: Nanotechnology comes into view. *Journal of Cellular Physiology*, *233*(12), 9223-9236.

42. Howley, B. V., & Howe, P. H. (2019). TGF-beta signaling in cancer: post-transcriptional regulation of EMT via hnRNP E1. *Cytokine*, *118*, 19-26.

43. Djediai, S., Gonzalez Suarez, N., El Cheikh-Hussein, L., Rodriguez Torres, S., Gresseau, L., Dhayne, S., ... & Annabi, B. (2021). MT1-MMP cooperates with TGF-β receptor-mediated signaling to trigger SNAIL and induce epithelial-to-mesenchymal-like transition in U87 glioblastoma cells. *International Journal of Molecular Sciences*, *22*(23), 13006.

44. Cristofanilli, M., Budd, G. T., Ellis, M. J., Stopeck, A., Matera, J., Miller, M. C., ... & Hayes, D. F. (2004). Circulating tumor cells, disease progression, and survival in metastatic breast cancer. *New England Journal of Medicine*, *351*(8), 781-791.

45. Aktas, B., Tewes, M., Fehm, T., Hauch, S., Kimmig, R., & Kasimir-Bauer, S. (2009). Stem cell and epithelial-mesenchymal transition markers are frequently overexpressed in circulating tumor cells of metastatic breast cancer patients. *Breast cancer research*, *11*(4), 1-9.

46. Al-Hajj, M., Wicha, M. S., Benito-Hernandez, A., Morrison, S. J., & Clarke, M. F. (2003). Prospective identification of tumorigenic breast cancer cells. *Proceedings of the National Academy of Sciences*, *100*(7), 3983-3988.

47. Cheung, K. J., Padmanaban, V., Silvestri, V., Schipper, K., Cohen, J. D., Fairchild, A. N., ... & Ewald, A. J. (2016). Polyclonal breast cancer metastases arise from collective dissemination of keratin 14-expressing tumor cell clusters. *Proceedings of the National Academy of Sciences*, *113*(7), E854-E863.

48. Aceto, N., Bardia, A., Miyamoto, D. T., Donaldson, M. C., Wittner, B. S., Spencer, J. A., ... & Maheswaran, S. (2014). Circulating tumor cell clusters are oligoclonal precursors of breast cancer metastasis. *Cell*, *158*(5), 1110-1122.

49. Zhou, B., Moodie, A., Blanchard, A. A., Leygue, E., & Myal, Y. (2015). Claudin 1 in breast cancer: new insights. *Journal of Clinical Medicine*, *4*(12), 1960-1976.

50. Gkountela, S., Castro-Giner, F., Szczerba, B. M., Vetter, M., Landin, J., Scherrer, R., ... & Aceto, N. (2019). Circulating tumor cell clustering shapes DNA methylation to enable metastasis seeding. *Cell*, *176*(1-2), 98-112.

51. Duda, D. G., Duyverman, A. M., Kohno, M., Snuderl, M., Steller, E. J., Fukumura, D., & Jain, R. K. (2010). Malignant cells facilitate lung metastasis by bringing their own soil. *Proceedings of the National Academy of Sciences*, *107*(50), 21677-21682.

52. Massagué, J., & Obenauf, A. C. (2016). Metastatic colonization by circulating tumour cells. *Nature*, *529*(7586), 298-306.

53. Wells, A., Yates, C., & Shepard, C. R. (2008). E-cadherin as an indicator of mesenchymal to epithelial reverting transitions during the metastatic seeding of disseminated carcinomas. *Clinical & experimental metastasis*, *25*(6), 621-628.

54. Chao, Y., Wu, Q., Acquafondata, M., Dhir, R., & Wells, A. (2012). Partial mesenchymal to epithelial reverting transition in breast and prostate cancer metastases. *Cancer Microenvironment*, *5*(1), 19-28.

55. Chao, Y. L., Shepard, C. R., & Wells, A. (2010). Breast carcinoma cells re-express E-cadherin during mesenchymal to epithelial reverting transition. *Molecular cancer*, *9*(1), 1-18.

56. Stankic, M., Pavlovic, S., Chin, Y., Brogi, E., Padua, D., Norton, L., ... & Benezra, R. (2013). TGF-β-Id1 signaling opposes Twist1 and promotes metastatic colonization via a mesenchymal-to-epithelial transition. *Cell reports*, *5*(5), 1228-1242.

57. Demirkan, B. (2013). The roles of epithelial-to-mesenchymal transition (EMT) and mesenchymal-to-epithelial transition (MET) in breast cancer bone metastasis: potential targets for prevention and treatment. *Journal of clinical medicine*, *2*(4), 264-282.

58. Almansour, N. (2022). Triple-Negative Breast Cancer: A Brief Review About Epidemiology, Risk Factors, Signaling Pathways, Treatment and Role of Artificial Intelligence. *Frontiers in Molecular Biosciences*, 32.

59. Anders, C. K., & Carey, L. A. (2009). Biology, metastatic patterns, and treatment of patients with triple-negative breast cancer. *Clinical breast cancer*, *9*, S73-S81.

60. Lin, N. U., Claus, E., Sohl, J., Razzak, A. R., Arnaout, A., & Winer, E. P. (2008). Sites of distant recurrence and clinical outcomes in patients with metastatic triple-negative breast cancer: high incidence of central nervous system metastases. *Cancer*, *113*(10), 2638-2645.

61. Terceiro, L. E., Edechi, C. A., Ikeogu, N. M., Nickel, B. E., Hombach-Klonisch, S., Sharif, T., ... & Myal, Y. (2021). The breast tumor microenvironment: A key player in metastatic spread. *Cancers*, *13*(19), 4798.

62. Anders, C. K., & Carey, L. A. (2009). Biology, metastatic patterns, and treatment of patients with triple-negative breast cancer. *Clinical breast cancer*, *9*, S73-S81.

63. Lv, Y., Ma, X., Du, Y., & Feng, J. (2021). Understanding patterns of brain metastasis in triple-negative breast cancer and exploring potential therapeutic targets. *OncoTargets and therapy*, *14*, 589.

64. Li, Y., Su, P., Wang, Y., Zhang, H., Liang, Y., Zhang, N., ... & Yang, Q. (2020). Impact of histotypes on preferential organ-specific metastasis in triple-negative breast cancer. *Cancer medicine*, *9*(3), 872-881.

65. Li, Y., Su, P., Wang, Y., Zhang, H., Liang, Y., Zhang, N., ... & Yang, Q. (2020). Impact of histotypes on preferential organ-specific metastasis in triple-negative breast cancer. *Cancer medicine*, *9*(3), 872-881.

66. Yin, L., Duan, J. J., Bian, X. W., & Yu, S. C. (2020). Triple-negative breast cancer molecular subtyping and treatment progress. *Breast Cancer Research*, *22*(1), 1-13.

67. Chang, J. W., Ding, Y., Tahir ul Qamar, M., Shen, Y., Gao, J., & Chen, L. L. (2019). A deep learning model based on sparse auto-encoder for prioritizing cancer-related genes and drug target combinations. *Carcinogenesis*, *40*(5), 624-632.

68. Won, K. A., & Spruck, C. (2020). Triple-negative breast cancer therapy: Current and future perspectives. *International journal of oncology*, *57*(6), 1245-1261.

69. Almansour, N. (2022). Triple-Negative Breast Cancer: A Brief Review About Epidemiology, Risk Factors, Signaling Pathways, Treatment and Role of Artificial Intelligence. *Frontiers in Molecular Biosciences*, 32.

70. Chalakur-Ramireddy, N. K., & Pakala, S. B. (2018). Combined drug therapeutic strategies for the effective treatment of Triple Negative Breast Cancer. *Bioscience reports*, *38*(1).

71. Davison, C., Morelli, R., Knowlson, C., McKechnie, M., Carson, R., Stachtea, X., ... & LaBonte, M. J. (2021). Targeting nucleotide metabolism enhances the efficacy of anthracyclines and anti-metabolites in triple-negative breast cancer. *NPJ breast cancer*, *7*(1), 1-13.

72. Yoshida, T., Ozawa, Y., Kimura, T., Sato, Y., Kuznetsov, G., Xu, S., ... & Matsui, J. (2014). Eribulin mesilate suppresses experimental metastasis of breast cancer cells by reversing phenotype from epithelial–mesenchymal transition (EMT) to mesenchymal–epithelial transition (MET) states. *British journal of cancer*, *110*(6), 1497-1505.

73. McKenna, M. T., Weis, J. A., Barnes, S. L., Tyson, D. R., Miga, M. I., Quaranta, V., & Yankeelov, T. E. (2017). A predictive mathematical modeling approach for the study of doxorubicin treatment in triple negative breast cancer. *Scientific reports*, *7*(1), 1-14.

74. Geenen, J. J., Linn, S. C., Beijnen, J. H., & Schellens, J. H. (2018). PARP inhibitors in the treatment of triple-negative breast cancer. *Clinical pharmacokinetics*, *57*(4), 427-437.

75. Yin, L., Duan, J. J., Bian, X. W., & Yu, S. C. (2020). Triple-negative breast cancer molecular subtyping and treatment progress. *Breast Cancer Research*, *22*(1), 1-13.

76. Nakhjavani, M., & Shigdar, S. (2022). Future of PD-1/PD-L1 axis modulation for the treatment of triple-negative breast cancer. *Pharmacological Research*, *175*, 106019.

77. Lotfinejad, P., Kazemi, T., Mokhtarzadeh, A., Shanehbandi, D., Niaragh, F. J., Safaei, S., ... & Baradaran, B. (2020). PD-1/PD-L1 axis importance and tumor microenvironment immune cells. *Life Sciences*, *259*, 118297

78. Thomas, R., Al-Khadairi, G., & Decock, J. (2021). Immune checkpoint inhibitors in triple negative breast cancer treatment: promising future prospects. *Frontiers in Oncology*, *10*, 600573.

79. Heimes, A. S., & Schmidt, M. (2019). Atezolizumab for the treatment of triple-negative breast cancer. *Expert opinion on investigational drugs*, *28*(1), 1-5.

80. Schettini, F., Giuliano, M., De Placido, S., & Arpino, G. (2016). Nab-paclitaxel for the treatment of triple-negative breast cancer: Rationale, clinical data and future perspectives. *Cancer treatment reviews*, *50*, 129-141.

81. Kwapisz, D. (2021). Pembrolizumab and atezolizumab in triple-negative breast cancer. *Cancer Immunology, Immunotherapy*, *70*(3), 607-617.

82. Gianni, L., Huang, C. S., Egle, D., Bermejo, B., Zamagni, C., Thill, M., ... & Viale, G. (2022). Pathologic complete response (pCR) to neoadjuvant treatment with or without atezolizumab in triple-negative, early high-risk and locally advanced breast cancer: NeoTRIP Michelangelo randomized study. *Annals of Oncology*, *33*(5), 534-543.

83. Bussard, K. M., Mutkus, L., Stumpf, K., Gomez-Manzano, C., & Marini, F. C. (2016). Tumor-associated stromal cells as key contributors to the tumor microenvironment. *Breast Cancer Research*, *18*(1), 1-11.

84. Hill, B. S., Sarnella, A., D'Avino, G., & Zannetti, A. (2020, February). Recruitment of stromal cells into tumour microenvironment promote the metastatic spread of breast cancer. In *Seminars in cancer biology* (Vol. 60, pp. 202-213). Academic Press.

85. Mbeunkui, F., & Johann, D. J. (2009). Cancer and the tumor microenvironment: a review of an essential relationship. *Cancer chemotherapy and pharmacology*, *63*(4), 571-582.

86. Alkasalias, T., Moyano-Galceran, L., Arsenian-Henriksson, M., & Lehti, K. (2018). Fibroblasts in the tumor microenvironment: shield or spear?. *International journal of molecular sciences*, *19*(5), 1532.

87. Jena, B. C., Sarkar, S., Rout, L., & Mandal, M. (2021). The transformation of cancer-associated fibroblasts: current perspectives on the role of TGF-β in CAF mediated tumor progression and therapeutic resistance. *Cancer Letters*, *520*, 222-232.

88. Luo, H., Tu, G., Liu, Z., & Liu, M. (2015). Cancer-associated fibroblasts: a multifaceted driver of breast cancer progression. *Cancer letters*, *361*(2), 155-163.

89. Yu, Y., Xiao, C. H., Tan, L., Wang, Q. S., Li, X. Q., & Feng, Y. (2014). Cancer-associated fibroblasts induce epithelial–mesenchymal transition of breast cancer cells through paracrine TGF-β signalling. *British journal of cancer*, *110*(3), 724-732.

90. Madu, C. O., Wang, S., Madu, C. O., & Lu, Y. (2020). Angiogenesis in breast cancer progression, diagnosis, and treatment. *Journal of Cancer*, *11*(15), 4474-4494.

91. Nagl, L., Horvath, L., Pircher, A., & Wolf, D. (2020). Tumor endothelial cells (TECs) as potential immune directors of the tumor microenvironment–New findings and future perspectives. *Frontiers in Cell and Developmental Biology*, 766.

92. Ohga, N., Ishikawa, S., Maishi, N., Akiyama, K., Hida, Y., Kawamoto, T., ... & Hida, K. (2012). Heterogeneity of tumor endothelial cells: comparison between tumor endothelial cells isolated from high-and low-metastatic tumors. *The American journal of pathology*, *180*(3), 1294-1307.

93. Bussolati, B., Assenzio, B., Deregibus, M. C., & Camussi, G. (2006). The proangiogenic phenotype of human tumor-derived endothelial cells depends on thrombospondin-1 downregulation via phosphatidylinositol 3-kinase/Akt pathway. *Journal of molecular medicine*, *84*(10), 852-863.

94. Graney, P. L., Tavakol, D. N., Chramiec, A., Ronaldson-Bouchard, K., & Vunjak-Novakovic, G. (2021). Engineered models of tumor metastasis with immune cell contributions. *Iscience*, *24*(3), 102179.

95. Müller, L., Tunger, A., Plesca, I., Wehner, R., Temme, A., Westphal, D., ... & Schmitz, M. (2020). Bidirectional crosstalk between cancer stem cells and immune cell subsets. *Frontiers in Immunology*, *11*, 140.

96. Qiu, S. Q., Waaijer, S. J., Zwager, M. C., de Vries, E. G., van der Vegt, B., & Schröder, C. P. (2018). Tumor-associated macrophages in breast cancer: Innocent bystander or important player?. *Cancer treatment reviews*, *70*, 178-189.

97. Aras, S., & Zaidi, M. R. (2017). TAMeless traitors: macrophages in cancer progression and metastasis. *British journal of cancer*, *117*(11), 1583-1591.

98. Chen, Y., Tan, W., & Wang, C. (2018). Tumor-associated macrophage-derived cytokines enhance cancer stem-like characteristics through epithelial–mesenchymal transition. *OncoTargets and therapy*, *11*, 3817.

99. Kitamura, T., Qian, B. Z., & Pollard, J. W. (2015). Immune cell promotion of metastasis. *Nature Reviews Immunology*, *15*(2), 73-86.

100. Fang, W., Zhou, T., Shi, H., Yao, M., Zhang, D., Qian, H., ... & Chen, T. (2021). Progranulin induces immune escape in breast cancer via up-regulating PD-L1 expression on tumor-associated macrophages (TAMs) and promoting CD8+ T cell exclusion. *Journal of Experimental & Clinical Cancer Research*, *40*(1), 1-11.

101. Ma, X., Wang, M., Yin, T., Zhao, Y., & Wei, X. (2019). Myeloid-derived suppressor cells promote metastasis in breast cancer after the stress of operative removal of the primary cancer. *Frontiers in oncology*, *9*, 855.

102. Weber, C. E., Kothari, A. N., Wai, P. Y., Li, N. Y., Driver, J., Zapf, M. A., ... & Mi, Z. (2015). Osteopontin mediates an MZF1–TGF-β1-dependent transformation of mesenchymal stem cells into cancer-associated fibroblasts in breast cancer. *Oncogene*, *34*(37), 4821-4833.

103. Olkhanud, P. B., Damdinsuren, B., Bodogai, M., Gress, R. E., Sen, R., Wejksza, K., ... & Biragyn, A. (2011). Tumor-Evoked Regulatory B Cells Promote Breast Cancer Metastasis by Converting Resting CD4+ T Cells to T-Regulatory CellsCancer-Promoting Role of B CellsCancer-Promoting Role of B Cells. *Cancer research*, *71*(10), 3505-3515.

104. Kuroda, H., Jamiyan, T., Yamaguchi, R., Kakumoto, A., Abe, A., Harada, O., & Masunaga, A. (2021). Tumor microenvironment in triple-negative breast cancer: the correlation of

tumor-associated macrophages and tumor-infiltrating lymphocytes. Clinical and Translational Oncology, 23(12), 2513-2525.

105. Kim, G., Pastoriza, J. M., Condeelis, J. S., Sparano, J. A., Filippou, P. S., Karagiannis, G. S., & Oktay, M. H. (2020). The contribution of race to breast tumor microenvironment composition and disease progression. *Frontiers in Oncology*, *10*, 1022.

106. Brassart-Pasco, S., Brézillon, S., Brassart, B., Ramont, L., Oudart, J. B., & Monboisse, J. C. (2020). Tumor microenvironment: extracellular matrix alterations influence tumor progression. *Frontiers in oncology*, *10*, 397.

107. Anderson, N. M., & Simon, M. C. (2020). The tumor microenvironment. *Current Biology*, *30*(16), R921-R925.

108. Pankov, R., & Yamada, K. M. (2002). Fibronectin at a glance. *Journal of cell science*, *115*(20), 3861-3863.

109. Fernandez-Garcia, B., Eiró, N., Marin, L., González-Reyes, S., Gonzalez, L. O., Lamelas, M. L., & Vizoso, F. J. (2014). Expression and prognostic significance of fibronectin and matrix metalloproteases in breast cancer metastasis. *Histopathology*, *64*(4), 512-522.

110. Qiao, P., & Lu, Z. R. (2020). Fibronectin in the tumor microenvironment. *Tumor Microenvironment*, 85-96.

111. Akiyama, S. K., Olden, K., & Yamada, K. M. (1995). Fibronectin and integrins in invasion and metastasis. *Cancer and Metastasis Reviews*, *14*(3), 173-189.

112. Lee, M. H., Ducheyne, P., Lynch, L., Boettiger, D., & Composto, R. J. (2006). Effect of biomaterial surface properties on fibronectin–α5β1 integrin interaction and cellular attachment. *Biomaterials*, *27*(9), 1907-1916.

113. Hannigan, G., Troussard, A. A., & Dedhar, S. (2005). Integrin-linked kinase: a cancer therapeutic target unique among its ILK. *Nature Reviews Cancer*, *5*(1), 51-63.

114. Utispan, K., Sonongbua, J., Thuwajit, P., Chau-In, S., Pairojkul, C., Wongkham, S., & Thuwajit, C. (2012). Periostin activates integrin α5β1 through a PI3K/AKT-dependent pathway in invasion of cholangiocarcinoma. *International journal of oncology*, *41*(3), 1110-1118.

115. Lin, T. C., Yang, C. H., Cheng, L. H., Chang, W. T., Lin, Y. R., & Cheng, H. C. (2019). Fibronectin in cancer: friend or foe. *Cells*, *9*(1), 27.

116. Stoeltzing, O., Liu, W., Reinmuth, N., Fan, F., Parry, G. C., Parikh, A. A., ... & Ellis, L. M. (2003). Inhibition of integrin α5β1 function with a small peptide (ATN-161) plus continuous 5-FU infusion reduces colorectal liver metastases and improves survival in mice. *International journal of cancer*, *104*(4), 496-503.

117. Cianfrocca, M. E., Kimmel, K. A., Gallo, J., Cardoso, T., Brown, M. M., Hudes, G., ... & Cohen, R. B. (2006). Phase 1 trial of the antiangiogenic peptide ATN-161 (Ac-PHSCN-NH2), a beta integrin antagonist, in patients with solid tumours. *British journal of cancer*, *94*(11), 1621-1626.

118. Shiu, R. P., & Iwasiow, B. M. (1985). Prolactin-inducible proteins in human breast cancer cells. *Journal of Biological Chemistry*, *260*(20), 11307-11313.

119. Haagensen Jr, D. E., Mazoujian, G., Dilley, W. G., Pedersen, C. E., Kister, S. J., & Wells Jr, S. A. (1979). Breast gross cystic disease fluid analysis. I. Isolation and radioimmunoassay for a major component protein. *Journal of the National Cancer Institute*, *62*(2), 239-247.

120. Calza, S., Hall, P., Auer, G., Bjöhle, J., Klaar, S., Kronenwett, U., ... & Pawitan, Y. (2006). Intrinsic molecular signature of breast cancer in a population-based cohort of 412 patients. *Breast Cancer Research*, *8*(4), 1-9.

121. Dawood, S., Hu, R., Homes, M. D., Collins, L. C., Schnitt, S. J., Connolly, J., ... & Tamimi, R. M. (2011). Defining breast cancer prognosis based on molecular phenotypes: results from a large cohort study. *Breast cancer research and treatment*, *126*(1), 185-192.

122. Lund, M. J., Butler, E. N., Hair, B. Y., Ward, K. C., Andrews, J. H., Oprea-Ilies, G., ... & Eley, J. W. (2010). Age/race differences in HER2 testing and in incidence rates for breast cancer triple subtypes: a population-based study and first report. *Cancer: Interdisciplinary International Journal of the American Cancer Society*, *116*(11), 2549-2559.

123. Murphy, L. C., Tsuyuki, D., Myal, Y., & Shiu, R. P. (1987). Isolation and sequencing of a cDNA clone for a prolactin-inducible protein (PIP). Regulation of PIP gene expression in the human breast cancer cell line, T-47D. *Journal of Biological Chemistry*, *262*(31), 15236-15241.

124. Fiel, M. I., Cernaianu, G., Burstein, D. E., & Batheja, N. (1996). Value of GCDFP-15 (BRST-2) as a specific immunocytochemical marker for breast carcinoma in cytologic specimens. *Acta cytologica*, *40*(4), 637-641.

125. Clark, J. W., Snell, L., Shiu, R. P. C., Orr, F. W., Maitre, N., Vary, C. P. H., ... & Watson, P. H. (1999). The potential role for prolactin-inducible protein (PIP) as a marker of human breast cancer micrometastasis. *British Journal of Cancer*, *81*(6), 1002-1008.

126. Baniwal, S. K., Chimge, N. O., Jordan, V. C., Tripathy, D., & Frenkel, B. (2013). Prolactin-induced protein (PIP) regulates proliferation of luminal A type breast cancer cells in an estrogen-independent manner. *PloS one*, *8*(6), e62361.

127. Naderi, A., & Vanneste, M. (2014). Prolactin-induced protein is required for cell cycle progression in breast cancer. *Neoplasia*, *16*(4), 329-342.

128. Hähnel R, Hähnel E. Expression of the PIP/GCDFP-15 gene and survival in breast cancer. Virchows Arch. 1996 Dec;429(6):365–9.

129. Pagani, A., Sapino, A., Bergnolo, P., Bussolati, G., & Eusebi, V. (1994). PIP/GCDFP-15 gene expression and apocrine differentiation in carcinomas of the breast. *Virchows Archiv*, *425*(5), 459-465.

130. Fritzsche, F. R., Thomas, A., Winzer, K. J., Beyer, B., Dankof, A., Bellach, J., ... & Kristiansen, G. (2007). Co-expression and prognostic value of gross cystic disease fluid protein 15 and mammaglobin in primary breast cancer. *Histology and histopathology*.

131. Jablonska, K., Grzegrzolka, J., Podhorska-Okolow, M., Stasiolek, M., Pula, B., Olbromski, M., ... & Dziegiel, P. (2016). Prolactin-induced protein as a potential therapy response marker of adjuvant chemotherapy in breast cancer patients. *American journal of cancer research*, *6*(5), 878.

132. Edechi, C. A., Ikeogu, N. M., Akaluka, G. N., Terceiro, L. E., Machado, M., Salako, E. S., ... & Myal, Y. (2021). The prolactin inducible protein modulates antitumor immune responses and metastasis in a mouse model of triple negative breast cancer. *Frontiers in Oncology*, 456.

133. Autiero, M., Abrescia, P., & Guardiola, J. (1991). Interaction of seminal plasma proteins with cell surface antigens: presence of a CD4-binding glycoprotein in human seminal plasma. *Experimental cell research*, *197*(2), 268-271.

134. Myal, Y., Robinson, D. B., Iwasiow, B., Tsuyuki, D., Wong, P., & Shiu, R. P. (1991). The prolactin-inducible protein (PIP/GCDFP-15) gene: cloning, structure and regulation. *Molecular and cellular endocrinology*, *80*(1-3), 165-175.

135. Hassan, M. I., Waheed, A., Yadav, S., Singh, T. P., & Ahmad, F. (2009). Prolactin inducible protein in cancer, fertility and immunoregulation: structure, function and its clinical implications. *Cellular and Molecular Life Sciences*, *66*(3), 447-459.

136. Mazoujian, G., Pinkus, G. S., Davis, S., & Haagensen Jr, D. E. (1983). Immunohistochemistry of a gross cystic disease fluid protein (GCDFP-15) of the breast. A marker of apocrine epithelium and breast carcinomas with apocrine features. *The American journal of pathology*, *110*(2), 105.

137. Myal, Y., & SHIU, R. C. (2000). The physiology and pathology of an apocrine protein: The prolactin-inducible protein (PIP)/gross cystic disease fluid protein (GCDFP-15). *Recent research developments in endocrinology*, 321-335.

138. Blais, Y., Gingras, S., Haagensen, D. E., Labrie, F., & Simard, J. (1996). Interleukin-4 and interleukin-13 inhibit estrogen-induced breast cancer cell proliferation and stimulate GCDFP-15 expression in human breast cancer cells. *Molecular and cellular endocrinology*, *121*(1), 11-18.

139. Blais, Y., Gingras, S., Haagensen, D. E., Labrie, F., & Simard, J. (1996). Interleukin-4 and interleukin-13 inhibit estrogen-induced breast cancer cell proliferation and stimulate GCDFP-15 expression in human breast cancer cells. *Molecular and cellular endocrinology*, *121*(1), 11-18.

140. Myal, Y., Iwasiow, B., Yarmill, A., Harrison, E., Paterson, J. A., & Shiu, R. P. (1994). Tissue-specific androgen-inhibited gene expression of a submaxillary gland protein, a rodent

homolog of the human prolactin-inducible protein/GCDFP-15 gene. *Endocrinology*, *135*(4), 1605-1610.

141. Osawa, M., Horiuchi, H., Tian, W., & Kaneko, M. (2004). Divergent evolution of the prolactin-inducible protein gene and related genes in the mouse genome. *Gene*, *325*, 179-186.

142. Lee, B., Bowden, G. H. W., & Myal, Y. (2002). Identification of mouse submaxillary gland protein in mouse saliva and its binding to mouse oral bacteria. *Archives of oral biology*, *47*(4), 327-332.

143. Zhou, W., & König, R. (2003). T cell receptor-independent CD4 signalling: CD4–MHC class II interactions regulate intracellular calcium and cyclic AMP. *Cellular signalling*, *15*(8), 751-762.

144. Autiero, M., Gaubin, M., Mani, J. C., Castejon, C., Martin, M., El Marhomy, S., ... & Piatier-Tonneau, D. (1997). Surface plasmon resonance analysis of gp17, a natural CD4 ligand from human seminal plasma inhibiting human immunodeficiency virus type-1 gp120-mediated syncytium formation. *European Journal of Biochemistry*, *245*(1), 208-213.

145. Hassan, M. I., Kumar, V., Singh, T. P., & Yadav, S. (2008). Purification and characterization of zinc α2-glycoprotein-Prolactin inducible protein complex from human seminal plasma. *Journal of separation science*, *31*(12), 2318-2324.

146. Caputo, E., Manco, G., Mandrich, L., & Guardiola, J. (2000). A novel aspartyl proteinase from apocrine epithelia and breast tumors. *Journal of Biological Chemistry*, *275*(11), 7935-7941.

147. Naderi, A., & Vanneste, M. (2014). Prolactin-induced protein is required for cell cycle progression in breast cancer. *Neoplasia*, *16*(4), 329-342.

148. Léon CPM, S., Johann, S., Els, W. W., Inge L, S. E., & Arie V, N. A. (1994). Identity of human extra parotid glycoprotein (EP-GP) with secretory actin binding protein (SABP) and its biological properties.

149. Schenkels, L. C., Rathman, W. M., Veerman, E. C., & Amerongen, A. V. N. (1991). Detection of proteins related to a salivary glycoprotein (EP-GP). Concentrations in human secretions (saliva, sweat, tears, nasal mucus, cerumen, seminal plasma).

150. Chiu, W. W. C., & Chamley, L. W. (2003). Human seminal plasma prolactin-inducible protein is an immunoglobulin G-binding protein. *Journal of reproductive immunology*, *60*(2), 97-111.

151. Kumar, S., Tomar, A. K., Singh, S., Saraswat, M., Singh, S., Singh, T. P., & Yadav, S. (2012). Human serum albumin as a new interacting partner of prolactin inducible protein in human seminal plasma. *International Journal of Biological Macromolecules*, *50*(2), 317-322.

152. Rashid, O. M., Nagahashi, M., Ramachandran, S., Dumur, C., Schaum, J., Yamada, A., ... & Takabe, K. (2014). An improved syngeneic orthotopic murine model of human breast cancer progression. *Breast cancer research and treatment*, *147*(3), 501-512.

153. Mendes, N., Dias Carvalho, P., Martins, F., Mendonça, S., Malheiro, A. R., Ribeiro, A., ... & Velho, S. (2020). Animal models to study cancer and its microenvironment. *Tumor Microenvironment*, 389-401.

154. Yamaguchi, R., & Perkins, G. (2018). Animal models for studying tumor microenvironment (TME) and resistance to lymphocytic infiltration. *Cancer Biology & Therapy*, *19*(9), 745-754.

155. Kessenbrock, K., Plaks, V., & Werb, Z. (2010). Matrix metalloproteinases: regulators of the tumor microenvironment. *Cell*, *141*(1), 52-67.

156. Mehner, C., Hockla, A., Miller, E., Ran, S., Radisky, D. C., & Radisky, E. S. (2014). Tumor cell-produced matrix metalloproteinase 9 (MMP-9) drives malignant progression and metastasis of basal-like triple negative breast cancer. *Oncotarget*, *5*(9), 2736.

157. Yang, B., Huang, J., Xiang, T., Yin, X., Luo, X., Huang, J., ... & Ren, G. (2014). Chrysin inhibits metastatic potential of human triple-negative breast cancer cells by modulating matrix metalloproteinase-10, epithelial to mesenchymal transition, and PI3K/Akt signaling pathway. *Journal of Applied Toxicology*, *34*(1), 105-112.

158. Shi, F., Xiao, F., Ding, P., Qin, H., & Huang, R. (2016). Long noncoding RNA highly up-regulated in liver cancer predicts unfavorable outcome and regulates metastasis by MMPs in triple-negative breast cancer. *Archives of Medical Research*, *47*(6), 446-453.

159. Chen, G., Yu, M., Cao, J., Zhao, H., Dai, Y., Cong, Y., & Qiao, G. (2021). Identification of candidate biomarkers correlated with poor prognosis of breast cancer based on bioinformatics analysis. *Bioengineered*, *12*(1), 5149-5161.

160. Helleman, J., Jansen, M. P., Ruigrok-Ritstier, K., van Staveren, I. L., Look, M. P., Meijer-van Gelder, M. E., ... & Berns, E. M. (2008). Association of an extracellular matrix gene cluster with breast cancer prognosis and endocrine therapy response. *Clinical cancer research*, *14*(17), 5555-5564.

161. Cassoni, P., Sapino, A., Haagensen, D. E., Naldoni, C., & Bussolati, G. (1995). Mitogenic effect of the 15-kDa gross cystic disease fluid protein (GCDFP-15) on breast-cancer cell lines and on immortal mammary cells. *International journal of cancer*, *60*(2), 216-220.

162. Baniwal, S. K., Chimge, N. O., Jordan, V. C., Tripathy, D., & Frenkel, B. (2013). Prolactin-induced protein (PIP) regulates proliferation of luminal A type breast cancer cells in an estrogen-independent manner. *PloS one*, *8*(6), e62361.

163. Zheng, Z., & Xie, X. (2013). Decreased prolactin-inducible protein expression exhibits inhibitory effects on the metastatic potency of breast cancer cells. *The Chinese-German Journal of Clinical Oncology*, *12*(3), 101-105.

164. Masuda, R., Semba, S., Mizuuchi, E., Yanagihara, K., & Yokozaki, H. (2010). Negative regulation of the tight junction protein tricellulin by snail-induced epithelial-mesenchymal transition in gastric carcinoma cells. *Pathobiology*, *77*(2), 106-113.

165. Kurrey, N. K., Amit, K., & Bapat, S. A. (2005). Snail and Slug are major determinants of ovarian cancer invasiveness at the transcription level. *Gynecologic oncology*, *97*(1), 155-165.

166. Plath, T., Detjen, K., Welzel, M., Von Marschall, Z., Murphy, D., Schirner, M., ... & Rosewicz, S. (2000). A novel function for the tumor suppressor p16INK4a: induction of anoikis via upregulation of the α5β1 fibronectin receptor. *The Journal of cell biology*, *150*(6), 1467-1478.

167. Yi, M., & Ruoslahti, E. (2001). A fibronectin fragment inhibits tumor growth, angiogenesis, and metastasis. *Proceedings of the National Academy of Sciences*, *98*(2), 620-624.

168. Fernandez-Garcia, B., Eiró, N., Marin, L., González-Reyes, S., Gonzalez, L. O., Lamelas, M. L., & Vizoso, F. J. (2014). Expression and prognostic significance of fibronectin and matrix metalloproteases in breast cancer metastasis. *Histopathology*, *64*(4), 512-522.

169. Malik, G., Knowles, L. M., Dhir, R., Xu, S., Yang, S., Ruoslahti, E., & Pilch, J. (2010). Plasma Fibronectin Promotes Lung Metastasis by Contributions to Fibrin Clots and Tumor

Cell InvasionPlasma Fibronectin Promotes Lung Metastasis. *Cancer research*, *70*(11), 4327-4334.

170. Humphries, M. J., Obara, M., Olden, K., & Yamada, K. M. (1989). Role of fibronectin in adhesion, migration, and metastasis. *Cancer investigation*, *7*(4), 373-393.

171. Schaffner, F., Ray, A. M., & Dontenwill, M. (2013). Integrin α5β1, the fibronectin receptor, as a pertinent therapeutic target in solid tumors. *Cancers*, *5*(1), 27-47.

172. Jin, Y. J., Park, I., Hong, I. K., Byun, H. J., Choi, J., Kim, Y. M., & Lee, H. (2011). Fibronectin and vitronectin induce AP-1-mediated matrix metalloproteinase-9 expression through integrin α5β1/αvβ3-dependent Akt, ERK and JNK signaling pathways in human umbilical vein endothelial cells. *Cellular signalling*, *23*(1), 125-134.

173. Morozevich, G., Kozlova, N., Cheglakov, I., Ushakova, N., & Berman, A. (2009). Integrin α5β1 controls invasion of human breast carcinoma cells by direct and indirect modulation of MMP-2 collagenase activity. *Cell cycle*, *8*(14), 2219-2225.

174. Weigelt, B., Geyer, F. C., & Reis-Filho, J. S. (2010). Histological types of breast cancer: how special are they?. *Molecular oncology*, *4*(3), 192-208.

175. Prat, A., Parker, J. S., Karginova, O., Fan, C., Livasy, C., Herschkowitz, J. I., ... & Perou, C. M. (2010). Phenotypic and molecular characterization of the claudin-low intrinsic subtype of breast cancer. *Breast cancer research*, *12*(5), 1-18.

176. Farmer, P., Bonnefoi, H., Becette, V., Tubiana-Hulin, M., Fumoleau, P., Larsimont, D., ... & Iggo, R. (2005). Identification of molecular apocrine breast tumours by microarray analysis. *Breast Cancer Research*, *7*(2), 1-1.

177. Lehmann, B. D., Bauer, J. A., Chen, X., Sanders, M. E., Chakravarthy, A. B., Shyr, Y., & Pietenpol, J. A. (2011). Identification of human triple-negative breast cancer subtypes and

preclinical models for selection of targeted therapies. *The Journal of clinical investigation*, *121*(7), 2750-2767.

178. Kurose, K., Hoshaw-Woodard, S., Adeyinka, A., Lemeshow, S., H. Watson, P., & Eng, C. (2001). Genetic model of multi-step breast carcinogenesis involving the epithelium and stroma: clues to tumour–microenvironment interactions. *Human molecular genetics*, *10*(18), 1907-1913.

179. Blanchard, A. A., Zelinski, T., Xie, J., Cooper, S., Penner, C., Leygue, E., & Myal, Y. (2016). Identification of claudin 1 transcript variants in human invasive breast cancer. *PLoS One*, *11*(9), e0163387.

180. Yao, Y., Chu, Y., Xu, B., Hu, Q., & Song, Q. (2019). Risk factors for distant metastasis of patients with primary triple-negative breast cancer. *Bioscience Reports*, *39*(6).

181. Dent, R., Trudeau, M., Pritchard, K. I., Hanna, W. M., Kahn, H. K., Sawka, C. A., ... & Narod, S. A. (2007). Triple-negative breast cancer: clinical features and patterns of recurrence. *Clinical cancer research*, *13*(15), 4429-4434.

182. Han, S., Khuri, F. R., & Roman, J. (2006). Fibronectin stimulates non–small cell lung carcinoma cell growth through activation of Akt/mammalian target of rapamycin/S6 kinase and inactivation of LKB1/AMP-activated protein kinase signal pathways. Cancer research, 66(1), 315-323.

183. Miller, F. R., Miller, B. E., & Heppner, G. H. (1983). Characterization of metastatic heterogeneity among subpopulations of a single mouse mammary tumor: heterogeneity in phenotypic stability. Invasion & metastasis, 3(1), 22-31.

184. Mathai, R. A., Vidya, R. V. S., Reddy, B. S., Thomas, L., Udupa, K., Kolesar, J., & Rao, M. (2019). Potential utility of liquid biopsy as a diagnostic and prognostic tool for the

assessment of solid tumors: implications in the precision oncology. Journal of clinical medicine, 8(3), 373.

185. Jhan, J. R., & Andrechek, E. R. (2017). Triple-negative breast cancer and the potential for targeted therapy. Pharmacogenomics, 18(17), 1595-1609.

186. Zhang, K., Corsa, C. A., Ponik, S. M., Prior, J. L., Piwnica-Worms, D., Eliceiri, K. W., ... & Longmore, G. D. (2013). The collagen receptor discoidin domain receptor 2 stabilizes SNAIL1 to facilitate breast cancer metastasis. Nature cell biology, 15(6), 677-687.

187. Favreau, A. J., Vary, C. P., Brooks, P. C., & Sathyanarayana, P. (2014). Cryptic collagen IV promotes cell migration and adhesion in myeloid leukemia. Cancer medicine, 3(2), 265-272.

188. Xu, S., Xu, H., Wang, W., Li, S., Li, H., Li, T., ... & Liu, L. (2019). The role of collagen in cancer: from bench to bedside. Journal of translational medicine, 17(1), 1-22.

189. Sevilla, C. A., Dalecki, D., & Hocking, D. C. (2010). Extracellular matrix fibronectin stimulates the self-assembly of microtissues on native collagen gels. Tissue Engineering Part A, 16(12), 3805-3819.

190. Kusuma, N., Denoyer, D., Eble, J. A., Redvers, R. P., Parker, B. S., Pelzer, R., ... & Pouliot, N. (2012). Integrin-dependent response to laminin-511 regulates breast tumor cell invasion and metastasis. International journal of cancer, 130(3), 555-566.

191. Zakout, Y. M. A., Abdullah, S. M., & Ali, M. A. (2012). Assessment of elastosis in invasive ductal carcinoma of the breast compared to fibroadenoma among Sudanese patients using conventional histochemical methods. Biotechnic & Histochemistry, 87(2), 122-125.

192. Wang, Y., Song, E. C., & Resnick, M. B. (2020). Elastin in the tumor microenvironment. Tumor Microenvironment, 1-16.

193. Silva, D., & Mesquita, A. (2022). Evolving Evidence for the Optimization of Neoadjuvant Therapy in Triple-Negative Breast Cancer. Breast Cancer: Basic and Clinical Research, 16, 11782234221107580.

194. Issa, A., Gill, J. W., Heideman, M. R., Sahin, O., Wiemann, S., Dey, J. H., & Hynes, N. E. (2013). Combinatorial targeting of FGF and ErbB receptors blocks growth and metastatic spread of breast cancer models. Breast Cancer Research, 15(1), 1-16.

195. Gauthier, B. R., Lorenzo, P. I., & Comaills, V. (2022). Physical Forces and Transient Nuclear Envelope Rupture during Metastasis: The Key for Success?. Cancers, 14(1), 83.

196. Navarro-Lerida, I., Pellinen, T., Sanchez, S. A., Guadamillas, M. C., Wang, Y., Mirtti, T., ... & Del Pozo, M. A. (2015). Rac1 nucleocytoplasmic shuttling drives nuclear shape changes and tumor invasion. Developmental cell, 32(3), 318-334.

197. Haimovici, A., Höfer, C., Badr, M. T., Bavafaye Haghighi, E., Amer, T., Boerries, M., ... & Häcker, G. (2022). Spontaneous activity of the mitochondrial apoptosis pathway drives chromosomal defects, the appearance of micronuclei and cancer metastasis through the Caspase-Activated DNAse. Cell Death & Disease, 13(4), 315.

198. Kwon, M., Leibowitz, M. L., & Lee, J. H. (2020). Small but mighty: The causes and consequences of micronucleus rupture. Experimental & Molecular Medicine, 52(11), 1777-1786.

199. Battaglia, R. A., Delic, S., Herrmann, H., & Snider, N. T. (2018). Vimentin on the move: new developments in cell migration. *F1000Research*, *7*.